WILEY-BLACKWELL AGU Books

The location of tropical precipitation and the hemispheric contrast of energy input to the atmosphere: why future tropical precipitation shifts are uncertain.

Journal:	*AGU Books*
Manuscript ID:	2015-Mar-CH-0290.R1
Wiley - Manuscript type:	Chapter
Date Submitted by the Author:	n/a
Complete List of Authors:	Donohoe, Aaron; University of Washington, Polar Science Center/ Applied Physics Lab Voigt, Aiko; Columbia University,
Primary Index Term:	1620 - Climate dynamics (0429 , 3309) < 1600 - GLOBAL CHANGE
Index Term 1:	3305 - Climate change and variability (1616 , 1635 , 3309 , 4215 , 4513) < 3300 - ATMOSPHERIC PROCESSES
Index Term 2:	1655 - Water cycles (1836) < 1600 - GLOBAL CHANGE
Index Term 3:	4532 - General circulation (1218 , 1222) < 4500 - OCEANOGRAPHY: PHYSICAL
Index Term 4:	3354 - Precipitation (1854) < 3300 - ATMOSPHERIC PROCESSES
Keywords:	intertropical convergence zone, global warming, hadley cell
Abstract:	The region of tropical convective precipitation (the ITCZ) migrates by approximately 12° of latitude over the seasonal cycle with an annual mean position slightly north of the equator. We demonstrate that the ITCZ is located in the hemisphere in which the atmosphere is heated more strongly and that the displacement of the ITCZ off the equator is proportional to the hemispheric contrast of atmospheric heating. A 3° latitude ITCZ shift requires approximately 1 PW of energy input into the atmosphere in one hemisphere with equal cooling in the other hemisphere. This relationship is shown to apply to the climatological seasonal cycle, the inter-annual variability and the response to both paleoclimatic and anthropogenic forcing. Future changes in the ITCZ position must conform the 3° latitude shift per PW of hemispherically asymmetric atmospheric heating. As a result, future changes in ITCZ position will likely be very small (<1° latitude) because hemispherically asymmetric forcings and climate feedbacks are small (<< 1 PW). Indeed, ensembles of coupled climate models simulate ITCZ shifts that are not significantly different from zero in response to an instantaneous quadrupling of carbon dioxide.

The location of tropical precipitation and the hemispheric contrast of energy input to the atmosphere: why future tropical precipitation shifts are uncertain.

Aaron Donohoe and Aiko Voigt

Abstract:

The region of tropical convective precipitation (the ITCZ) migrates by approximately 12° of latitude over the seasonal cycle with an annual mean position slightly north of the equator. We demonstrate that the ITCZ is located in the hemisphere in which the atmosphere is heated more strongly and that the displacement of the ITCZ off the equator is proportional to the hemispheric contrast of atmospheric heating. A 3° latitude ITCZ shift requires approximately 1 PW of energy input into the atmosphere in one hemisphere with equal cooling in the other hemisphere. This relationship is shown to apply to the climatological seasonal cycle, the inter-annual variability and the response to both paleoclimatic and anthropogenic forcing.

Future changes in the ITCZ position must conform the 3° latitude shift per PW of hemispherically asymmetric atmospheric heating. As a result, future changes in ITCZ position will likely be very small (<1° latitude) because hemispherically asymmetric forcings and climate feedbacks are small (<< 1 PW). Indeed, ensembles of coupled climate models simulate ITCZ shifts that are not significantly different from zero in response to an instantaneous quadrupling of carbon dioxide.

1. Introduction

The contrast between the moist tropics and dry subtropics is a fundamental feature of the climate system and is a consequence of the mass overturning circulation of the atmosphere. Solar heating of the low-latitudes causes upward atmospheric motion near the equator resulting in a region of convective precipitation (Figure 1A). The upward mass flux does not penetrate above the stable tropopause but, instead, diverges horizontally giving rise to poleward flow aloft. Eastward deflection of the poleward wind by the Coriolis force in the upper branch of the circulation results in the Westerly subtropical jets and also demands a meridional temperature gradient via thermal wind balance. The latter becomes baroclinically unstable for a meridionally expansive circulation and thus, the meridional extent of the poleward flow aloft is limited by the simultaneous constraints of conservation of angular momentum and thermal wind balance (Held, 1980). Mass converges aloft on the poleward side of the Hadley circulation resulting in subsidence and dry surface conditions associated with the subtropics. Thus, the contrast between the dry subtropics and moist tropics is intimately related to the strength, position and width of the atmospheric mass overturning circulation in the tropics – commonly referred to as the Hadley cell (Hadley, 1735).

Patterns of tropical precipitation and dryness have wide-spread biological and socio-economic impacts. The moist tropics are home to some of the most rich and diverse species of flora and fauna on the planet (Koppen, 1936) whereas the subtropical deserts are amongst the most sparsely populated regions of the planet due to their lack of biodiversity and water resources. Inter-annual variations in tropical precipitation have large implications for agricultural production, especially in the semi-arid regions where water resources are marginal (Sivakumar, 2005). Thus, understanding future changes in the position, intensity and width of the Hadley cell and its associated impact on large scale patterns of precipitation climatology and variability is of critical importance to society. Moreover, the Hadley cell is part of the global circulation of the atmosphere and changes in the strength and location of the Hadley cell have the potential to

change tropical cyclones (Vimont and Kossin, 2007; Merlis et al. 2013) and extratropical jetstreams (Ceppi et al. 2013)

Here we focus on the processes that determine the location of the region of intense tropical precipitation in the tropical rainbelt on seasonal and longer timescales. In the Northern Hemisphere (NH) summer, the regions of most intense precipitation (blue lines in Figure 1B) are located North of the equator with an intense band of precipitation around 6-10° N in the Pacific and extending out to beyond 15°N over the land domain, especially in the Indian monsoon. During the Southern Hemisphere (SH) summer, a zonal band of precipitation in the Tropical Pacific remains north of the equator but has de-intensified significantly. A North-West to South-East tilted band of precipitation in the South Tropical Pacific – the South Pacific Convergence Zone (SPCZ) -- has emerged as the region of most intense precipitation (Figure 1C). The annual mean precipitation map represents a smoothed and smeared version of the seasonally migrating regions of intense precipitation that follow the sun.

While zonal inhomogeneities in precipitation, including the monsoonal systems, are prevalent and important from both societal and meteorological perspectives, we will focus here on the pattern of zonal mean precipitation that defines the tropical-subtropical contrast and its relationship to the Hadley cell. In the Boreal summer, the zonal mean precipitation maximum (left Panel of Figure 1B) is clearly in the Northern Hemisphere, with its magnitude of 8 mm/day exceeding the subtropical precipitation minimum by a factor of 4. During the Austral summer, the zonal mean precipitation clearly peaks South of the Equator although there is a remnant of the precipitation maximum North of the equator seen during the Boreal summer. In all seasons, the maximum precipitation is co-located with the ascending branch of the Hadley circulation (left panels of figure 1) – where the meridional gradient of the mass overturning circulation is greatest. In the annual mean, the upward motion and convective precipitation are co-located with the zero in the streamfunction. However, during both solstices, there is a prevalent magnitude asymmetry between the winter and summer Hadley cells, with the winter cell intensifying by approximately a factor of 3 relative to its annual mean (c.f. the left panels of Figure 1A to those in 1B-C) while the summer Hadley cell all but disappears. As a result of this amplitude asymmetry between the winter and summer Hadley cell, the maximum upward velocities and precipitation are located within the winter Hadley cell and equatorward of the zero streamfunction.

While the literature sometimes distinguishes between the zonal band of precipitation in Tropical North Pacific and the SPCZ precipitation, here we treat the precipitation in the two regions as a single entity: the seasonally migrating convective precipitation associated with the upwelling branch of the Hadley circulation (left panels of Figure 1). We refer to the location of the zonal mean precipitation maximum as the intertropical convergence zone (ITCZ), so named for the horizontal convergence of winds in the lower atmosphere that give rise to the upward atmospheric motion and convective precipitation. We note that the region of convective precipitation that we use to define the ITCZ here is inseparable from the low level convergence since convection (upward motion in the atmosphere) demands low level convergence for an incompressible fluid (Boussinesq continuity equation) subject to the boundary condition of no vertical flow through the surface. The annual mean precipitation is best thought of as a statistical average of a seasonally bi-modal spatial distribution of precipitation, with regions of intense precipitation prevalent north of the Equator in the Pacific, in the SPCZ region and also in the monsoons of India, South-East Asia, Australia and Northern Africa. In this regard, the annual mean precipitation and Hadley cell (Figure 1A) represents a physical state that is seldom

realized, just as the mean of a sine curve is unlikely to occur and merely represents the average of a bi-modal distribution (which happens to be symmetric about the mean in the case of a pure sine curve). While the annual mean precipitation is definitely skewed Northward off the equator, we demonstrate below that the annual mean ITCZ position represents the small residual of seasonal ITCZ migrations off the equator that are an order of magnitude larger than the annual mean.

The co-location of the ITCZ and the ascending branch of the Hadley circulation demands that the atmosphere moves energy away from the hemisphere in which the ITCZ is located with the energy export proportional to ITCZ displacement off the equator. This relationship results from the following properties of the tropical atmospheric circulation as summarized in Figure 2A:

1. Because the upper branch of the Hadley circulation flows from the ascending to descending branches, the upper level mass flux at the equator is away from the ITCZ

2. Conservation of mass requires that there is equal mass flux in the upper and lower branch of the Hadley circulation and, therefore, the net moisture and energy fluxes at the equator will be in the direction of the mass flux at the vertical level of the moisture and energy maxima

3. The total energy of an air parcel is equal to the moist static energy (MSE):

$$MSE = Lq + C_P T + gZ \quad , \qquad (1)$$

where L is the latent heat of vaporization of water vapor, q is the specific humidity, C_p is the heat capacity of air at constant pressure, T is the temperature, g is the acceleration of gravity and Z is the height above sea level. While both moisture (q) and temperature (T) achieve their (tropospheric) maxima at or near the surface, the increase in geopotential (gZ) with altitude generally exceeds the decrease in the sum of latent (Lq) and sensible energies ($C_P T$), resulting in MSE increasing with altitude. If this was not true, the atmospheric column as a whole would be unstable to moist convection. As a result of this combined with point (2) above, the net energy flux across the equator is away from the ITCZ. This logic neglects the role of transient and stationary eddy energy transport which are generally an order of magnitude smaller than that associated with the mass overturning circulation in the deep tropics (Held, 2001).

4. In contrast to energy, moisture content maximizes at the surface. Thus the net moisture flux is in the sense of the surface mass flux, is toward the ITCZ (Frierson et al. 2013) and provides the moisture convergence required for precipitation exceeding evaporation within the ITCZ region.

5. The streamfunction magnitude at the equator will increase as the ITCZ moves farther off the equator. Provided that changes in the bulk moist stability do not change appreciably with the ITCZ shift, the energy flux across the equator is away from the ITCZ and is proportional to the ITCZ displacement off the equator.

The atmosphere moves 2.1 PW of energy from North to South across the (green arrow and labeling in the Left panel of Figure 1B) equator during the Boreal summer which is associated with a counter-clockwise mass overturning circulation of approximately 170 Sv (1 Sv is a Sverdrup mass flux equivalent of 10^9 kg S^{-1}). In the opposite season, the mass overturning circulation and atmospheric energy flux at the equator have reversed direction with comparable but slightly smaller amplitude; the atmosphere moves 1.9 PW of energy South to North across the equator associated with a 140 Sv, clockwise mass overturning circulation. Overall, the seasonal variations in energy transport across the equator are incredibly highly correlated with the mass overturning streamfunction at the equator ($R^2 = 0.99$) with a regression coefficient that implies a 14K contrast in the moist potential temperature ($\approx MSE/C_P$) between the Northward and Southward flowing air in the Hadley cell (Donohoe et al. 2013b). Given the observed moist stability of the tropics, the above 14K contrast suggest an average vertical separation of 600hPa between the equatorward and poleward mass flux which is (as expected) slightly smaller than the observed ~800 hPa deep circulation. This result implies that seasonal variations on the moist stability of the tropics and atmospheric energy transport exert a secondary influence on the inter-hemispheric energy transport as compared to variations in the strength and location of the Hadley cell.

A negative correlation between atmospheric energy transport across the equator (hereafter AHT_{EQ}) and ITCZ location is therefore expected based on the prominent dynamics in the deep tropics. But is this relationship useful or merely diagnostic? Since the energy storage in the atmospheric column is small, AHT_{EQ} must be balanced by a hemispheric contrast of energy input to the atmosphere by way of either the radiation at the top of atmosphere (TOA) or surface energy fluxes. Therefore, the relationship between ITCZ location and AHT_{EQ} allows one to relate the ITCZ location to the hemispheric-scale atmospheric energy budget. Provided the physics that relate the ITCZ location to the Hadley cell and energy transport are robust and climate state invariant, this relationship between the ITCZ and large-scale energy budget of the climate system will apply not only to the seasonal cycle but across all time scales including the response to external forcing. We will demonstrate that the $ITCZ_{LOC}/AHT_{EQ}$ ratio is robust and consistent across timescales in both models and observations including: 1. the annual mean climatology, 2. the seasonal cycle, 3. the inter-annual variability and 4. the response to external forcing, including both paleoclimatic and anthropogenic forcing. This theory for the ITCZ location and the hemispheric energy budget allows us to understand the magnitude and direction of future ITCZ shifts from the large scale patterns of climate forcings and feedbacks and their uncertainties. As such we will need a quantitative relationship between ITCZ location and AHT_{EQ}. In Section 2 we present empirical estimates of this relationship across timescales and also discuss the energetic processes that give rise to a hemispheric contrast of energy input to the atmosphere. In Section 3, we address the physical processes that control the value of the $ITCZ_{LOC}/AHT_{EQ}$ relationship and relate the amplitude of seasonal ITCZ migrations to the annual mean ITCZ location and the meridional extent of tropical convective precipitation. We then extend these results to the changes in tropical precipitation expected under global warming (Section 4).

2. The relationship between ITCZ position and hemispheric contrast of atmospheric heating

We previously argued that the ITCZ is co-located with the ascending branch of the Hadley cell, which results in cross-equatorial atmospheric energy transport away from the hemisphere in which the ITCZ is located. In this section, we demonstrate that the atmospheric energy transport across the equator (AHT_{EQ}) is a good proxy for the ITCZ location ($ITCZ_{LOC}$) across a myriad of timescales with the approximate relationship:

$$ITCZ_{LOC} \approx -3\ (^\circ\ PW^{-1})\ AHT_{EQ} \quad . \qquad (2)$$

The negative sign in Equation (2) means that an $ITCZ_{LOC}$ in the NH (+) is associated with Southward (-) energy transport across the equator and vice-versa. The factor of $3\ ^\circ\ PW^{-1}$ suggests that, if the ITCZ shifted 3° of latitude the associated atmospheric circulation would export 1 PW ($=10^{15}$ W) away from the hemisphere to which the ITCZ has shifted. This translates to a heating of 4 W m^{-2} averaged over a single hemisphere with equal cooling in the opposite hemisphere. To put that number in perspective, one would have to simultaneously double CO_2 in one hemisphere and halve CO_2 in the other hemisphere in order to achieve the same climate forcing. We emphasize that the factor of $3^\circ\ PW^{-1}$ is an approximate relationship that seems to hold for many model simulations and applications but there is no a priori reason to expect this quantitative relationship; it is intended more as a guide for understanding the magnitude of forcing and energetic feedback processes needed for a given ITCZ shift. We argue that it is difficult to achieve a hemispheric asymmetry of climate forcing and/or climate response of this magnitude (~1PW) and, thus, the $ITCZ_{LOC}$ appears to be a relatively stable feature of the climate system with changes greater than a couple degrees of latitude rather unlikely even under rather extreme climate forcing such as those associated with glacial cycles.

The atmospheric energy transport across the equator is fundamentally a consequence of the hemispheric contrast of atmospheric heating; in order to move energy from the NH to the SH, there must be a source of atmospheric heating in the NH. In the introduction to this section, we derive the relationship between AHT_{EQ} and the hemispheric energy budget for the annual mean climatology which we will later extend to other timescales. By way of equation (2), we can then quantitatively relate the ITCZ location --including its variability and future changes-- to the hemispheric energy budget. This is the goal of this chapter.

In the annual mean, the ascending branch of the Hadley cell and ITCZ are located in the NH (Figure 1A) which results in Southward AHT_{EQ} in the Hadley circulation. The hemispheric energy budget demands a spatially integrated atmospheric heating equal to AHT_{EQ} and an equal magnitude atmospheric cooling in the SH. This heating can either be provided by a net radiative heating at the TOA or by way of the surface energy fluxes from the ocean to the atmosphere:

$$-AHT_{EQ} = \langle NET_{RAD} \rangle + \langle SHF \rangle \quad , \qquad (3)$$

where brackets denote the spatial integrals over the NH, NET_{RAD} is the net radiative heating at the TOA and SHF is the surface energy flux defined as positive to the atmosphere. Global energy balance requires that the global integral of NET_{RAD} and SHF is zero in order for the energy budget of the climate system as a whole and surface to be in steady state. Therefore, Equation (3) could also be defined from the spatial integrals of NET_{RAD} and SHF over the SH with signs

reversed[1]. In simple terms, the net heating of the atmosphere in either hemisphere must be balanced by energy export across the equator and an equal magnitude of cooling in the opposite hemisphere.

The annual mean net energy flux from the surface to the atmosphere is a consequence of ocean heat transport convergence provided the ocean energy content is stable (i.e. at the climatological time scale). Therefore, the climatological hemispheric energy budget in Equation (3) can be rewritten as:

$$-AHT_{EQ} = \langle NET_{RAD} \rangle + OHT_{EQ} \quad , \qquad (4)$$

since the ocean heat transport convergence spatially integrated over either hemisphere is equal to the heat transport across the border, in this case the equator (Figure 2A). Moving the OHT_{EQ} term on the right hand side of the equator to the left results in the statement that the coupled (atmosphere plus ocean) energy export across the equator is balanced by net radiative heating/cooling of the hemispheres.

In this Section we explore the terms in the hemispheric energy budget (Equations 3 and 4) and the implication for the $ITCZ_{LOC}$ via Equation (2).

2.1. Annual mean ITCZ location

The annual mean ITCZ location north of the equator is associated with a Hadley cell that is shifted into the NH (Figure 1A) and 0.2±0.1PW of Southward AHT_{EQ} (Marshall et al. 2013). The latter demands an equivalent magnitude of atmospheric heating in the NH via Equation 4 which is accomplished by the surface energy fluxes by way of the large-scale oceanic circulation (OHT_{EQ}) transporting 0.4±0.2 PW northward across the equator and an opposing net radiative cooling ($\langle NET_{RAD} \rangle$) of the NH that is smaller in magnitude (-0.2±0.1 PW – Figure 2B). The atmospheric and oceanic energy transports across the equator oppose each other and the ITCZ position in the NH would not be energetically possible without the oceanic circulation and, more specifically, the energy transport in the Atlantic Meridional Overturning Circulation (AMOC -- Frierson et al. 2013). This conclusion is based on the fact that the net radiation at the TOA heats the SH and cools the NH and, acting alone, would favor an ITCZ in the SH. We explore the processes leading to the hemispheric contrast of radiative heating below.

The annual mean insolation is completely symmetric about the equator. Therefore, any hemispheric contrast in absorbed shortwave radiation (ASR) – the net shortwave radiation at the TOA—is a consequence of differences in the planetary albedo of the two hemispheres. Voigt et al. (2013) recently demonstrated that the two hemispheres have identical planetary albedos. This result is perhaps surprising given that the predominance of land in the NH is associated with a larger surface albedo in the NH than the SH. However, the Southern ocean is very cloudy which results in more shortwave reflection in the mid-latitudes of the SH as compared to the same latitudes in the NH (Donohoe and Battisti 2011). The NH is slightly (1.24 K) warmer than the SH (Kang et al. 2014). Consistent with the temperature dependence of longwave emission by the Stefan Boltzman law, the NH emits more (0.8 W m^{-2}) outgoing longwave radiation (OLR) than the SH resulting in a net radiative cooling of the NH of 0.2 PW.

[1] For the case of a global mean disequilibrium, the global mean imbalances can be removed prior to the calculation of the hemispheric mean or, equivalently, half the difference between the SH and NH integrals can be taken. For the purposes here, we have also neglected the atmospheric energy storage which is, in general, small but non-negligible on seasonal time scales.

How well do coupled climate models simulate the hemispheric contrast of energy input into the climate system and ITCZ location? As a metric for the ITCZ location we use the centroid of zonal mean precipitation (P_{CENT}) equatorward of 20° defined as the latitude for which there are equal amounts of precipitation between the regions from P_{CENT} to 20N and from P_{CENT} to 20S (Frierson and Hwang 2012). Figure 3a shows that the ensemble of CMIP3 coupled preindustrial simulations (Meehl et al. 2007) simulate a wide range of ITCZ locations and AHT_{EQ}. Despite the wide range of ITCZ locations simulated in the models, including three in the SH, the inter-model spread in ITCZ location is well correlated with the AHT_{EQ} as would be expected based on the mutual dependence of $ITCZ_{LOC}$ and AHT_{EQ} on the Hadley cell location. Thus, the model bias and spread in ITCZ location appears to be a consequence of the failure of the models to simulate the hemispheric scale energy budget discussed in the previous paragraph. In particular, model differences and an ensemble average bias in the planetary albedo over the Southern ocean explain the inter-model spread and model bias toward a more southward positioned ITCZ (Hwang and Frierson, 2013); this result suggests that the well-known double ITCZ bias in climate models is primarily a consequence of too much ASR in the SH resulting in a net heating of the SH atmosphere and, thus, an ITCZ in the SH with associated northward AHT_{EQ}.

We note that the slope of the linear best fit to the inter-model spread in Figure 3A is -3.2 ± 0.7 ° PW^{-1}. We will demonstrate that the approximate quantitative relationship between $ITCZ_{LOC}$ and AHT_{EQ} of -3 ° PW^{-1} holds not only for the inter-model differences in the annual mean climatology but also for many timescales and experiments. We note that the observations (blue square in Figure 3A) fail to fall on this line within the observational uncertainty. We believe, however, that the "failure" of the observed annual mean climatology to fit on this line does not necessarily contradict the hypothesis of a universal $ITCZ_{LOC}/AHT_{EQ}$ slope because the observed annual mean AHT_{EQ} is complicated by several issues including: 1. the AHT_{EQ} in the annual mean Hadley cell differs drastically between reanalysis products (Marshall et al. 2013) due to differences in reanalysis products at the top of the tropical boundary layer, 2. there is a significant energy flux in the stratosphere in the observations that is poorly constrained by measurements and 3. stationary waves make a significant contribution to the annual mean AHT_{EQ} in the observations (Heaviside and Czaja 2013) and not in the models.

2.2. Seasonal cycle of ITCZ location and AHT_{EQ}

The zonal mean ITCZ is displaced farthest North (7.3°N) in August and farthest South (5.3°S) in February (Figure 3B) with an annual mean position (1.6°N) that reflects the small asymmetry between the northward and southward seasonal migration off the equator. Seasonal variations in the ITCZ location and AHT_{EQ} are incredibly well correlated ($R^2 = 0.99$) with a regression coefficient of -2.7 ± 0.6 ° PW^{-1} (Figure 3B). This relationship again suggests that a 3° latitude ITCZ shift is accompanied by 1 PW of energy exchange between the two hemispheres, which must be accompanied by the same quantity of atmospheric heating/cooling in each hemisphere. Coupled climate models show remarkably similar relationships between the seasonal cycle of ITCZ location and AHT_{EQ} both in terms of the order 3° latitude ITCZ shift per PW of AHT_{EQ} (c.f. the slopes of the thin dashed lines and thick solid blue line in Fig. 3B) and the amplitude of the seasonal cycle of ITCZ location (Donohoe et al. 2013b) suggesting that the physical processes relating the mutual dependence of ITCZ location and AHT_{EQ} to the Hadley cell are robust in models and Nature alike. We note that a nearly identical (-2.9° PW^{-1}) seasonal

relationship between the ITCZ location and AHT_{EQ} is found if the ITCZ location is defined as the centroid of precipitation over the ocean domain only, suggesting that the amplitude of the seasonal migration of the ITCZ is unaffected by the alternating monsoons of Asia and Australia.

Seasonal variations in the hemispheric contrast of energy input to the atmosphere (and therefore AHT_{EQ} and $ITCZ_{LOC}$) are driven by changes in the meridional distribution of insolation. The latter causes the ASR contrast between the two hemispheres to vary by 22 PW seasonally as measured by the amplitude of annual harmonic. Less than 10% of the seasonal variations in energy input into each hemisphere is fluxed to the opposite hemisphere while approximately 75% is stored within the ocean, 8% is stored within the atmosphere and 7% is emitted back to space as OLR. It is unsurprising that the majority of seasonal variations in radiation at the TOA are stored in the ocean since the majority of the ASR passes through the atmosphere and is absorbed by the surface. The ocean has a large heat capacity and therefore takes some time to heat up before it fluxes energy upwards to the atmosphere via latent and sensible energy fluxes and, thus, most of the solar insolation absorbed at the surface never finds its way into the atmospheric column on seasonal timescales. But why only 10% of the seasonal variations in insolation are fluxed across the equator is an outstanding question in climate science. Surely the climate system would be very different if this percentage was altered significantly.

The seasonal migration of the Hadley cell and ITCZ off the equator is the climate system's response to hemispherical asymmetric insolation. Because the seasonal insolation forcing is large compared to any external forcing (i.e. anthropogenic or paleoclimatic), the robust relationship between ITCZ location and the hemispheric contrast of atmospheric heating over the seasonal cycle (in both observations and models) provides a constraint to how the system responds to internal variability and external forcing. We will further argue that the same quantitative relationship of 3° latitude ITCZ shift per PW of AHT_{EQ} discussed here applies to all time scales because ITCZ shifts at longer time scales can be viewed as small modifications of the climatological seasonal cycle and, therefore, are well approximated by linearizations about the seasonal cycle.

2.3. Interannual variability of ITCZ location

The ITCZ location varies interannually by of order 1° (2σ of annual mean variability = 0.7°) with approximately twice as much variability at the monthly timescale. We focus here on the annual mean anomalies which have a more robust connection to Hadley cell anomalies. The inter-annual variability of the ITCZ location and AHT_{EQ} over the satellite era show the expected negative correlation (Figure 3C). A northward ITZC displacement is associated with an intensification of the climatological Hadley cell with anomalous precipitation North of the equator in the upwelling branch of the Hadley cell and decreased precipitation south of the equator in the region of anomalous subsidence (Donohoe et al. 2014a). A 1° northward ITCZ shift is associated with 0.34 PW of southward AHT_{EQ} in the enhanced counterclockwise Hadley circulation at the equator. This result is consistent with the approximately 3° latitude ITCZ shift per PW of AHT_{EQ} seen in the previous two sections. We note that the correlation between El Nino—the prominent mode of East-West sea surface temperature variability in the Tropical Pacific—and both the ITCZ location and AHT_{EQ} is not significant although recent literature suggests that the correlation is significant in the Boreal winter (Adam et al. 2015).

What processes contribute to interannual variations in the heating of the NH atmosphere at the expense of the SH leading to a northward ITCZ shift? The lack of a consistent observing

network preclude an evaluation of the observed hemispheric energy budget but we can evaluate the processes at play in a coupled climate model displaying similar interannual statistics between $ITCZ_{LOC}$ and AHT_{EQ}. In the GFDL climate model (AM2.1), anomalous heating of the NH atmosphere is associated with positive net radiative anomalies in the Northern Tropics which appear to be a positive feedback from the ITCZ shift itself. The northward shifted deep-convective clouds reflect additional shortwave radiation but also emit less OLR since the cloud tops are higher and colder. The reduced ASR and OLR in the ITCZ region partially cancel each other but the OLR reduction is larger in magnitude leading to a radiative gain in the region the ITCZ has shifted to. This mechanism provides a positive feedback to any initial ITCZ shift since the radiative gain must be balanced by more AHT_{EQ} away from the ITCZ and, hence, a further ITCZ shift in same direction. Voigt et al. (2014) found this mechanisms to be important in other climate models as well, but also showed that its magnitude and even its sign (positive or negative feedback) depends on how models represent the coupling between tropical clouds and tropical circulation. It also remains unclear how important this mechanism is in the observed climate system.

Alternative mechanisms of hemispherically asymmetric climate variability (i.e. those leading to ITCZ shifts) include: 1. Variations in the OHT_{EQ} including decadal variations in the Atlantic Meridional Overturning Circulation (AMOC) 2. extratropical cloud radiative feedbacks and 3. the expansion of sea (or land) ice in a single hemisphere. These mechanisms have yet to emerge as a source of significant ITCZ variability in either climate model simulations or the observed record. Our quantitative scaling between ITCZ shifts and the hemispheric energy budget allows us to assess the impact some of these mechanisms might have on the ITCZ shift. For example, the basic state OHT_{EQ} is approximately 0.5 PW and is primarily associated with the AMOC. Some models produce interannual variations in the AMOC that are approximately 20% of the climatological mean circulation. Less than half of that variability (<10% of total) persists at time scales of variability longer than a year. If the entirety of that variability was realized as 0.05 PW of compensating southward AHT_{EQ}, the associated ITCZ shift would be 0.15° or less than 20 km ITCZ shift, likely in the noise of an observation network and well below the horizontal resolution of a global climate model. This is likely an upper bound of the impact of the AMOC energy transport on the ITCZ since much of the AMOC energy transport is stored in the deep ocean, even at the decadal scale, and some portion of the AMOC heating anomaly will be radiated to space as an OLR anomaly. Thus, the AHT_{EQ} will compensate for but be significantly smaller in magnitude than the initial OHT_{EQ}. Similarly, the impact of cloud and surface albedo anomalies on the interannual variability of the ITCZ can be estimated from the impact of each on the variability of the hemispheric average planetary albedo over the satellite era. Monthly anomalies in the hemispheric average planetary albedo from the satellite observations (Kato et al. 2006, Voigt et al. 2013) lead to single hemisphere heating anomalies of that are smaller in magnitude (1σ) than 0.1 PW with atmospheric contributions to planetary albedo contributing < 0.09 PW and surface contributions to planetary albedo contributing < 0.03 PW. Together, these estimates suggest that the inter-annual variability of planetary albedo has a small hemispheric asymmetry that would contribute to ITCZ migrations of less than 50 km if acting in isolation with no other feedbacks (Voigt et al. 2013).

2.4. ITCZ shift due to external forcing

We now consider the annual mean ITCZ shift due to external forcing. We argue that the approximate relationship of 3° latitude ITCZ shift per PW of AHT_{EQ} which we saw for the

annual mean climatology, seasonal cycle and interannual variability also applies to the annual mean ITCZ shift. Therefore, understanding how forcing mechanisms and climate feedbacks project onto the hemispheric energy budget allows one to predict the magnitude and direction of the ITCZ shift. Here we consider different coupled climate model forcings in conjunction to emphasize that the aforementioned scaling of ITCZ shifts can be generalized to many climate states: 1. 1% CO_2 increase per year to doubling (hereafter $2XCO_2$), 2. the Last glacial maximum (LGM), 3. the mid-Holocene, 4. freshwater hosing experiments to shut down the AMOC circulation and 5. a transient climate simulation running from the LGM to present day. We will see that the ITCZ shift is small (~1° latitude) for all climate forcing seen here because it is hard to realize a hemispheric contrast of atmospheric heating of more than a couple tenths of a PW even when considering fairly large climate forcings such as the introduction of the Laurentide ice sheet to the NH.

The change in ITCZ location and AHT_{EQ} in all experiments is shown in Figure 3D, with each cross representing a different model simulation color coded by the experiment type (see labeling inset). The ITCZ response to each forcing experiment differs drastically between the different climate models. The ensemble average shift in the LGM and $2XCO_2$ simulations is not significantly different from zero while the Northward shift in the mid-Holocene is marginally significant (95% confidence interval). The inter-model spread in ITCZ shift is strongly correlated with the change in AHT_{EQ} ($R = -0.84$) with a regression coefficient of $-3.2° \text{ PW}^{-1}$ when considering all forcing experiments collectively. This result again suggests that both the ITCZ location and AHT_{EQ} are mutually dependent on the Hadley cell location for all climate states. Furthermore, the order 3° latitude ITCZ shift per PW of energy transport suggests that the same dependence between the ITCZ, AHT_{EQ} and Hadley cell found over the seasonal cycle, annual mean climatology and inter-annual variability also determine the response to external forcing, implying that the bulk stability of the tropics and the relationship between the location of the upwelling branch of the Hadley circulation and the value of the mass overturning streamfunction at the equator is nearly climate state invariant. Most importantly, this result suggests that if we had a theory for how climate forcing and feedbacks project onto the hemispheric energy budget, we could make a quantitative prediction for the change in the ITCZ location[2]. Furthermore, the ITCZ shift is fairly small ($<1^o$) in all simulations because the shift is constrained to the approximately 3^o PW^{-1} relationship and the change in the hemispheric contrast of energy input to the atmosphere does not exceed 0.3 PW even for the highly hemispherically asymmetric forcing associated with the Laurentide ice sheet in the LGM. We briefly discuss the change in the hemispheric atmospheric energy budget in the LGM experiments, the processes leading to the inter-model spread below and a comparison of the model results to paleoclimatic proxy records below. A more extensive analysis of the simulated ITCZ due to CO_2 forcing is provided in Section 4.

The LGM simulations are forced by a prescribed land ice topography that features a large Laurentide ice sheet in the NH (Peltier, 2004) with more modest ice sheet enhancement in the SH. Overall, the surface albedo of the NH increases by approximately 0.03 relative to that of the SH in the ensemble average. Surprisingly, the ensemble average response to LGM boundary

[2] Some portion of the hemispheric asymmetry in energy input to the atmosphere may be a consequence of the ITCZ shift itself, either due to radiative changes associated with shifting convection or changes in surface fluxes associated with ocean circulation anomalies initiated by changing trade winds. These effects can be incorporated into a predictive model for ITCZ shifts – in response to an energy input external to the ITCZ shift—by introducing a feedback gain associated with the energetic changes due to the ITCZ shift as discussed in Donohoe et al. (2014a).

conditions and forcing is not significantly different from zero despite the large and hemispherically asymmetric forcing. If the change in surface albedo was realized at the TOA, the energy input to the NH would decrease by 1.3 PW, which we would extrapolate to a 4° southward ITCZ shift provided that the energy deficit was balanced by a compensating northward AHT_{EQ} . We explain below why the ensemble average ITCZ shift is so much smaller in these simulations and why the ITCZ even shifts northward in two of the models below.

In order for the surface albedo to make an impact in the TOA radiation budget (and therefore the atmospheric energy budget) solar radiation must be transmitted downward through the atmosphere, be reflected by the surface albedo, and then get transmitted back to the TOA. Therefore, the surface contribution to planetary albedo should *scale* as the atmospheric transmissivity squared (Donohoe and Battisti 2011). Approximately 20% of insolation is absorbed within the atmospheric column – primarily by ozone and water vapor. 25% of the insolation is reflected back to space – primarily off the top of clouds. Therefore, the atmospheric shortwave transmissivity is approximately 0.55 which means that a 3 unit change in surface albedo will translate to a 1 unit change in planetary albedo and the atmospheric energy budget. In the LGM case the atmosphere is slightly more shortwave transparent than the present day and the anticipated deficit of energy to the NH 1.3PW based on changes in surface albedo alone is reduced to 0.6PW when accounting for the atmospheric transmissivity squared. Furthermore, cloud cover is reduced over the Laurentide ice sheet, which causes a 0.17 PW heating of the NH atmosphere resulting in a net shortwave deficit of 0.43PW when added to the surface albedo impact. The NH cools relative to the SH, which causes a reduction of OLR by 0.32 PW via the Planck feedback. Thus, the ensemble average total radiative deficit of the NH is 0.11 PW and the resulting change in the AHT_{EQ} is accomplished by a small (~0.2°) southward ITCZ shift. The key point of the above analysis is that the anticipated energy deficit of the NH induced by the ice sheet albedo (of order 1.3 PW) is ameliorated by the basic state atmospheric transmissivity, cloud feedbacks and the Planck feedback to produce a very modest (of order 0.1 PW) change in the energy input to the NH, a modest AHT_{EQ} anomaly and, thus, a small ITCZ shift. We see that radiative feedbacks act to partially balance any hemispherically asymmetric forcing. This results in an ITCZ position that is a fairly stable property of the climate system.

In the two LGM simulations where the ITCZ shifts northward, radiative feedbacks and changes in ocean circulation result in an ITCZ shift that differs in direction from that anticipated from the forcing alone. In one simulation (MPI ECHAM5), the Planck feedback associated with the cooling of the NH exceeds the decrease in ASR in the NH. As a result, the introduction of the Laurentide ice sheet acts as a source of energy to the NH in part because the high topography (upwards of 5km) causes the surface to cool and emit less OLR. The other model with a Northward ITCZ shift during the LGM simulation (IAP-FGOALS) has nearly compensating changes in the SW cooling and longwave warming due to the introduction of the Laurentide ice sheet to the NH. However, the model shows a significant increase in the northward OHT_{EQ} that results in a compensating southward AHT_{EQ} and northward ITCZ shift. These cases emphasize that the hemispheric asymmetry of radiative feedbacks can result in an ITCZ shift whose sign is questionable even in the presence of a hemispherically asymmetric forcing.

2.4.3. ITCZ shifts from paleo-proxy records

Much effort has gone into reconstructing past changes in the position and intensity of the ITCZ using proxy data thought to reflect changes in hydrology or wind strength.

These include records of vegetation, lake water balance, precipitation isotopes, river sediment discharge, surface ocean isotopes, and marine primary productivity. Together, these records suggest the following ITCZ shifts over the paleo-history of the Earth:

1. a southward shift of the ITCZ relative to its modern position during the LGM (Arbuszewski et al. 2013)

2. a further, rapid southward shift of the ITCZ associated with a proposed AMOC shutdown during Heinrich events when there is widespread evidence of North Atlantic cooling (Peterson et al. 2000) and an equally abrupt northward shift during the Bølling Allerød when there evidence that the AMOC circulation reinvigorated

3. a northward ITCZ shift in the mid-Holocene (Haug et al. 2001) especially during the Boreal summer as deduced from the presence of lakes in the now arid Sahara (deMenocal *et al. 2000)*

4. a southward ITCZ shift during the little ice age (1400-1850) in the Tropical Pacific (Sachs et al. 2009)

Multi-proxy reconstructions suggest a simultaneous moistening of sites north of the modern day ITCZ location and drying of sites south of the modern day ITCZ during northward ITCZ shifts, which greatly strengthens the interpretation of the results. However, most studies can only give a qualitative ITCZ shift. More specifically, because the climatological precipitation decreases between the ITCZ location and the subtropical precipitation minimum at approximately 20°, any meridional translational of the ITCZ of less than 20° latitude will result in concurrent precipitation changes of opposite signs north and south of the ITCZ. Do the ITCZ shifts deduced above correspond to small (<1°) ITCZ shifts similar to those seen in the climate models or to shifts of order 10° as have been claimed in the literature based on the notion that the ITCZ itself must migrate over a location in order to moisten the region?

Recent work has used paleo SST reconstructions alongside observational estimates of the relationship between tropical SST gradients to begin to answer the above question. Similar to the relationship between AHT_{EQ} and the ITCZ location, the ITCZ position is also strongly correlated with SST contrast (ΔSST) between the northern tropics (0-20°N) and southern tropics (0-20°S) with the ITCZ moving towards the warmer SSTs. The regression coefficient between ITCZ position and SST contrast is approximately 2° per K (Donohoe et al 2013b) and is nearly invariant with timescale (i.e. similar statistics hold for the seasonal cycle in observations and models, the inter-annual variability and the response to external forcing). Paleo reconstructions of tropical SSTs from isotopic analysis allow a calculation of ΔSST during the LGM (23-19 kyears before present), Heinrich event 1 (HS1, 17-15 kyears before present) and the mid-Holocene (7-5kyears before present). The latter can be used alongside the relationships between ΔSST, ITCZ location and AHT_{EQ} to place the modeling results presented here in the context of the observational estimates (shaded circles and hatched uncertainties in Figure 3D). While there is considerable uncertainty in the proxy reconstructions (the dashed lines extend across the zero

axis suggesting the estimates are not significantly different than zero) the climate model ensemble average ITCZ shift and change in AHT_{EQ} for the LGM and mid-Holocene are in excellent agreement with the proxy estimates (c.f. the shaded green and blue squares with the shaded circles of the same color). We emphasize here not the correspondence of the numbers from the modeling simulations and the proxy records but, rather, that the small magnitude of the ITCZ shifts seen in the modeling studies is validated by the proxy records. More specifically, no model simulation produces an ITCZ shift of greater than 1° latitude and the proxy evidence is inconsistent with ITCZ shifts of greater than 1° for all time periods considered here even when accounting for the uncertainties in the proxy SST reconstructions and the relationships between ITCZ location and ΔSST. Models and observational evidence thus suggest that the ITCZ location is fairly stable in time. We emphasize, however, that the above discussion is limited to the annual zonal-mean ITCZ location and that regional changes to which proxy records are sensitive to–especially those associated with monsoons—are not subject to the same constraints.

The energetic framework for ITCZ shifts suggests that a complete shutdown of the AMOC would cause a fairly modest (~1°) southward ITCZ shift. The AMOC carries approximately 0.5 PW of energy Northward across the equator (Frierson et al. 2013). Therefore, a complete AMOC shutdown would result in an anomalous southward AHT_{EQ} of 0.5 PW provided that there were no radiative feedbacks, which is likely an upper bound given that radiative heating of the NH would most likely result in more OLR via the Planck feedback. This anomalous AHT_{EQ} would demand a 1.5° southward ITCZ shift given our scaling of 3° PW^{-1} for a complete AMOC shutdown. Indeed, model simulations of both the modern day and LGM system forced by (unrealistically large) freshwater input to the Atlantic (Chiang and Bitz 2005) result in an approximate 50% weakening of the AMOC and simulate a 0.5° southward ITCZ (purple outlined diamonds in Figure 3D) shift, with a 0.15 PW increase in AHT_{EQ} that is in very good agreement with the logic above for a halving of AMOC strength. Additionally, the proxy evidence from HS1, a time when the AMOC strength was thought to be severely reduced due to iceberg freshwater input to the North Atlantic, indicate a southward ITCZ shift of order 0.6° (purple circle in 3D), which also agrees with the magnitude of the changes anticipated from models and theory. Overall, the balance of evidence suggests that a complete AMOC shutdown would result in an ITCZ shift of around 1° latitude.

2.5. ITCZ response to climate forcing over the last 23,000 years

He at al. (2010) recently simulated the transient climate evolution (TraCE) of the last 23,000 years in a coupled simulation with the NCAR CCSM3 model. This simulation is forced by time-evolving orbital parameters, greenhouse gases and prescribed land ice topography from reconstructions. Additionally, freshwater forcing of the Atlantic is applied during times when paleo proxy data suggests iceberg discharges and a slowdown of the AMOC circulation. This simulation gives a plausible reconstruction of the LGM climate, the deglaciation, abrupt NH cooling associated with HS1 and the Younger Dryas, the rapid warming into the Bølling Allerød and the rather quiescent and stable climate of the Holocene in a single, continuous simulation (Liu et al. 2009). We use this simulation to illustrate the magnitude and mechanisms of ITCZ shifts over the recent paleo history of the Earth.

The ITCZ location varies by approximately 2° latitude (red lines in Figure 4A) from its southernmost location during HS1 (17-15 kyears ago) to its northernmost location during the early Bølling Allerød (14,500 years ago)[3]. The ITCZ location and AHT_{EQ} changes are nearly locked to each other for all time periods and transitions (c.f. the red and blue lines in Figure 4A). We have multiplied the AHT_{EQ} axis (right, blue axis in Figure 4A) by the factor of -3° latitude PW^{-1} for ease of comparison. We see that the same relationship between ITCZ location and AHT_{EQ} that was found over the observed seasonal cycle, interannual variability, the model spread in climatological mean state and response to external forcing also applies to the transient transitions in the TraCE simulation. We now ask: what physical processes influence the direction and magnitude of the hemispheric contrast in energy input to the atmosphere and therefore dictate the ITCZ shift via changes in AHT_{EQ}?

The southward AHT_{EQ} is decomposed into changes in the net radiative heating of the NH ($<NET_{RAD}>$) and heating of the NH by way of the OHT_{EQ} (and subsequent surface energy fluxes) via equation 4. Decadal averages are shown in Figure 4B which are sufficiently long to allow changes in atmospheric and oceanic energy content to be ignored and, hence, the near equality of <SHF> and OHT_{EQ}. As expected, the OHT_{EQ} is reduced by approximately 0.3 PW after the freshwater pulse heading into HS1 (around 17,500 years ago) followed by a recovery and overshoot beyond the modern day value during the Bølling Allerød after the freshwater forcing has been removed (14,500 years ago). A similar reduction and subsequent recovery of smaller magnitude is observed during the Younger Dryas (13 kyears ago) when the applied freshwater forcing is smaller in magnitude. The OHT_{EQ} reduction is consistent with an approximately 50% reduction in the strength of the AMOC circulation. The partial shutdown of the AMOC triggers Arctic sea-ice expansion that reduces $<NET_{RAD}>$ by approximately half the magnitude of the change in OHT_{EQ} via the positive ice albedo feedback. The longer term upward trend in NET_{RAD} is associated with the poleward retreat of snow and ice cover in the NH moving toward the present, including the retreat of the Laurentide ice sheet. Over the entirety of the simulation, there is more variance in the radiative input of energy into the NH than that in OHT_{EQ} despite the visually apparent abrupt transitions in the AMOC circulation; the decadal average range (2σ) of $<NET_{RAD}>$ is 0.28 PW compared to 0.16 PW for OHT_{EQ}.

The TraCE results emphasize that the 3° ITCZ per PW of (differential) energy input into the NH atmosphere holds across time scale and climate state and that understanding the magnitude and sign of ITCZ shifts relies on understanding how climate forcing and feedbacks impact the hemispheric contrast of energy input to the atmosphere. The very extreme freshwater forcing of HS1 leads to approximately a 0.3 PW reduction of AMOC strength (slightly amplified by the ice albedo feedback), whereas the melting of the Laurentide ice sheet results in an enhancement of the radiative input into the NH of 0.4 PW at the 10,000 year timescale. All in all, the total forcing and feedbacks on the hemispheric scale are of order 0.7 PW which results in ITCZ variability of approximately 2°. This variability is associated with the deglaciation, arguably one of the most extreme climate transitions our planet has seen in its more recent past. These numbers thus likely set an upper bound on the anticipated future changes in the zonal-mean ITCZ position due to anthropogenic forcing.

3. Relationship between the seasonal cycle of ITCZ migration and the annual mean precipitation distribution

[3] We note the CCSM3 has a basic state ITCZ bias with an ITCZ slightly south of the equator. This bias is a consequence of enhanced ASR in the Southern Ocean due to reduced cloud reflection relative to the observations.

What processes determine the quantitative relationship between ITCZ location and AHT_{EQ} of 3° latitude per PW? If the annual mean Hadley cell were simply meridionally translated alongside the ITCZ, the change in AHT_{EQ} would be approximately equal to the meridional gradient of AHT evaluated at the equator (a first order Taylor expansion) times the meridional ITCZ shift. The annual mean AHT has a gradient of approximately 0.1 PW per ° at the equator. Therefore this conceptual model projects that the ITCZ should shift by 10° latitude per PW of AHT_{EQ}, which is a sensitivity approximately 3 times greater than what we found from observations and models in the previous section. A similar formulation for ITCZ sensitivity to energy input based on the net energy input into the tropical atmosphere was recently expanded on by Schneider et al. (2014).

Why is the ITCZ three times less sensitive to the hemispheric contrast in forcing and feedbacks than the conceptual model based on the meridional translation of the annual mean climatology above suggest? We argue that the large seasonal migrations of the Hadley cell and ITCZ render the annual mean a less meaningful physical state that is seldom realized in the real (or modeled) climate system. As a result, a linearization about the annual mean state provides unrealistic ITCZ sensitivity to external forcing due to the exclusion of a seasonal cycle. Specifically, the magnitude asymmetry between the winter and summer Hadley cells that is present in the seasonal extremes but not in the annual mean (c.f. Figure 1 B and C with figure 1A) causes the quantitative relationship between the ITCZ and AHT_{EQ} to differ fundamentally between the annual mean and seasonal extremes for two reasons:

1. In the annual mean, the ITCZ and maximum upward velocities are co-located with the zero streamfunction of the Hadley circulation due to the near symmetry of the Hadley circulation about the ITCZ. In contrast, the magnitude asymmetry between the winter and summer Hadley cells during the seasonal extremes results in maximum upward velocity and ITCZ location where the meridional gradient of the streamfunction is greatest. Thus, during the course of the seasonal cycle, the ITCZ is located within the winter Hadley cell and equatorward of the zero streamfunction

2. The intensification of the winter Hadley cell as the ITCZ moves away from the equator toward the seasonal extremes results in a stronger mass overturning circulation at the equator than would be expected if the Hadley cell simply translated meridionally (Lindzen and Hou, 1988).

As a result of the above mechanisms, the ITCZ shift off the equator is smaller than the Hadley cell shift (via 1) and the AHT_{EQ} changes more than would be expected from the meridional translation of the annual mean Hadley cell (via 2). Both mechanisms cause the ITCZ location to be less sensitive to a hemispheric contrast of energy input relative to the linearization about the annual mean state. Why these mechanisms reduce the ITCZ sensitivity by a factor of 3 is an outstanding question in climate dynamics.

In this section, we expand on the relationship between the seasonal cycle of the ITCZ location and the annual mean response to external forcing (Section 3.1) and how the amplitude of the seasonal cycle of the ITCZ determines the meridional extent of tropical convective precipitation (Section 3.2).

3.1. Annual mean ITCZ shifts and the seasonal cycle

The annual mean ITCZ location, Hadley cell and AHT_{EQ} are the small residual of large seasonal migrations of the Hadley cell off the equator. Here we demonstrate that annual mean changes in the ITCZ location represent small changes in the duration or amplitude of the seasonal migrations of the ITCZ off the equator and, as a result, the seasonal relationship between ITCZ location and AHT_{EQ} determines the same relationship for the annual mean ITCZ shift. Figure 4C shows smoothed seasonal histograms of the ITCZ location and AHT_{EQ} for the 2 thousand year periods centered on the (blue) LGM , (gray) HS1, the (green) mid-Holocene and (red) modern (shaded bars of the same color in Figure 4A-B) in the TraCe simulations. As we noted for the observed seasonal cycle (Section 2B), the ITCZ and AHT_{EQ} are most often found in a seasonal extreme position with the ITCZ located around 5° N (S) and with a corresponding southward (northward) AHT_{EQ} of – (+) 2 PW. The annual mean ITCZ location and AHT_{EQ} (open circles) are seldom realized and represent the statistical average of the seasonal modes. As such, the annual mean $ITCZ_{LOC}$ and AHT_{EQ} lies on the line connecting the seasonal modes, which has the slope of approximately 3° PW^{-1}.

The differences in the seasonal histograms of $ITCZ_{LOC}$ and AHT_{EQ} across the different paleoclimate epochs in TraCE are fairly modest. More specifically, in all states the system is most likely to be in a seasonal mode and the relationship between $ITCZ_{LOC}$ and AHT_{EQ} over the seasonal cycle is consistently 3° PW^{-1} in all climate states. We speculate that this result holds because the seasonal heating of the atmosphere induced by the seasonal migration of the sun is much larger in magnitude than any external forcing such that the perturbations to the seasonal cycle are small compared to the amplitude of the basic state seasonal cycle. We do see small variations in the duration of the seasonal modes and the magnitude of the ITCZ displacement off the equator during the seasonal modes across the different paleoclimate epochs. Changes in the seasonal ITCZ modes can cause annual mean ITCZ shifts via 3 possible mechanisms:

1. Equatorward/poleward shifts during a single season. As an example: the most poleward migration of the ITCZ in the Boreal summer during the LGM is nearly identical to that of the modern but the ITCZ migrates farther poleward during the Austral summer (c.f. the blue and red contours in the lower right quadrant of Figure 4C). As a result, there is an annual mean southward ITCZ shift.

2. Opposing equatorward/poleward shifts during both seasons. As an example: during HS1 the ITCZ migrates less far off the equator during the Boreal summer as compared to the LGM and the ITCZ migrates farther off the equator during the Austral summer (c.f. the gray and blue contours in both the lower right and upper left quadrants). As a result, there is an annual mean southward ITCZ shift.

3. Changes in the duration of the season. As an example, during the mid-Holocene, the ITCZ spends less time in the Boreal summer mode and more time in the Austral summer mode as compared to the modern (c.f. the relative areas of the red and green contours in the upper left and lower right quadrants). This mechanism shifts the annual mean ITCZ toward the more frequently occupied mode—to the south in this case. In the mid-Holocene, there is a simultaneous poleward ITCZ shift of the Boreal summer ITCZ mode which nearly cancels the contribution above. We note that the concurrent intensification and shortening of the duration of the Boreal summer with near zero net effect matches the precessional forcing during the mid-Holocene which has zero annual mean due to Kepler's second law.

We note that simultaneous poleward or equatorward ITCZ shifts during both seasons (symmetric stretching/compression) cancel each other in the annual mean and have little impact on the annual mean ITCZ location. We return to the implication of this mode of variability on the meridional extent of the tropics in the next subsection.

In all cases, because the annual mean ITCZ shift is a consequence of small variations in the seasonality of the ITCZ migration off the equator, *the change in annual mean ITCZ location and AHT_{EQ} must follow the seasonal relationship between the ITCZ and AHT_{EQ}*. For the reasons discussed in the introduction to this section, the 3° ITCZ shift per PW of AHT_{EQ} over the seasonal cycle is approximately a factor of 3 less than would be expected from a linearization about the annual mean climatology. Given the robustness of the mutual dependence of ITCZ location and AHT_{EQ} on the seasonal migration of the Hadley cell off the equator, we would anticipate future changes in the ITCZ location to be governed by the hemispheric contrast of climate forcing and feedbacks according to the 3° latitude ITCZ shift per PW AHT_{EQ}.

3.2. The meridional extent of tropical convective precipitation and the amplitude of the seasonal cycle

The distinction between the moist tropics and dry subtropics is fundamentally set by the prevailing vertical motion in the atmosphere associated with the upwelling and downwelling branches of the Hadley circulation respectively. The annual mean meridional profile of precipitation represents the smearing out of many instantaneous realizations of intense and localized precipitation that migrate in time over the seasonal cycle. Therefore, the meridional extent of the region of tropical convective precipitation is a consequence of how far off the equator the ITCZ moves. Here, we think of the width of the tropical precipitation as roughly corresponding to the region of ascending atmospheric motion that extends from the mass overturning streamfunction minimum at the equatorward edge of the SH subtropics to the streamfunction maximum at the equatorward edge of the NH subtropics. We note that this metric of the width of tropical precipitation is independent of the mean ITCZ position.

As an illustration of the connection between the seasonal migration of the ITCZ and the width of tropical convective precipitation, we examine the impact of seasonal migrations of the ITCZ off the equator on the meridional profile of annual mean precipitation in an ensemble of slab ocean aquaplanet simulations – an atmosphere coupled to a motionless ocean. We modify the amplitude of the seasonal cycle by changing the ocean depth from 2.4 m to 50 m. In the deeper runs, more of the seasonal variations in insolation are stored within the ocean and never enter the atmospheric column to impact the atmospheric temperature and circulation (Donohoe et al. 2013a). In the shallower ocean simulations, the intensification of the insolation in the summer hemisphere rapidly heats up the ocean which subsequently fluxes energy upward to the atmosphere to drive a large seasonal cycle of atmospheric temperature and energy input to the atmosphere. As a result, there is a much larger hemispheric contrast of energy input to the atmosphere and, hence, larger AHT_{EQ} during the solstices in the shallow ocean runs than the deep ocean runs (c.f. the orange lines in Figure 5C-D). The larger AHT_{EQ} is accomplished by strongly displacing the Hadley cell off the equator, resulting in a large mass overturning circulation at the equator (gray contours in Figure 5D) and an ITCZ in the summer hemisphere (blue lines). In contrast, in the deep ocean simulations, the Hadley cell and ITCZ barely move off the equator during the solstice seasons. In these runs, hemispheric symmetry demands that the annual mean ITCZ and Hadley cells are centered on the equator.

The impact of the amplitude of seasonal migrations of the ITCZ off the equator on the annual mean precipitation is truly profound. In the 50 m ocean depth simulation, the ITCZ hardly moves seasonally. Thus the annual mean precipitation looks much like the seasonal extremes with a well-defined region of intense precipitation confined to within 10° of the equator and an intense Hadley cell comparable in magnitude to the circulation during the solstices (Figure 5A). In contrast, the large seasonal migration of the Hadley cell in the 2.4 m simulations results in the meridional smearing out of the convective precipitation over a meridional broad region; there is almost no precipitation contrast between the tropics and extratropics (Figure 5B). Similarly, the time averaging of large seasonal variations in the Hadley circulation results in a small time averaged streamfunction at any location; the regions of annual mean upward and downward atmospheric motion are not well defined. The meridional extent of tropical convective precipitation is fundamentally set by the seasonal migration of the ITCZ off the equator which is demanded by the seasonal energy input into the atmosphere.

As discussed in Section 2B, only 10% of the seasonal variations in the hemispheric contrast of ASR are realized as AHT_{EQ}. Therefore, the potential for climate forcing and feedbacks to change the amplitude of the seasonal cycle of atmospheric heating, and hence the meridional width of tropical convective precipitation, is immense. In general, the moistening of the atmosphere tends to amplify the seasonal cycle of atmospheric heating (Donohoe and Battisti 2014), the melting of sea ice diminishes the seasonal energy input to the atmosphere (Dwyer, 2012) while emission of sulfate aerosols diminish (Hwang et al. 2013) and those of black carbon enhance (Allen et al 2014) the seasonal cycle of atmospheric heating. Overall, understanding how climate forcing and feedbacks impact the seasonal amplitude of energy input to the atmosphere and thus the meridional width of the Hadley cell (Johanson and Fu 2009) and tropical convective precipitation is a fundamental challenge for global climate change forecasts.

4. Implications for future ITCZ shifts under global warming

How does anthropogenic forcing lead to a hemispheric contrast of energy input to the atmosphere and, thus, meridional ITCZ shifts? Climate forcing by atmospheric constituents with residence times that are shorter than the inter-hemispheric transport timescale (1-2 years – Bowman and Cohen, 1997) are localized to the region (hemisphere) of emission. For example, sulfate aerosol emissions are overwhelmingly in the NH and, thus, lead to a reduction in ASR in the NH. Therefore, we would expect the ITCZ to shift southward in response to sulfate aerosol emissions. Indeed, the observational record and climate model simulations of the past century both show a southward ITCZ shift during the 1980s when sulfate aerosol emissions from India peaked. Other anthropogenic forcing agents that are spatially localized (e.g. land use change, black carbon accumulation on ice, etc.) are also expected to directly force ITCZ shifts and we can use the approximate 3^{o} latitude PW^{-1} of spatially integrated forcing as a rough (neglecting feedback processes) guide to the magnitude of the associated ITCZ shifts.

Here, we focus on the ITCZ shifts induced by well mixed (i.e. long-lived) forcing agents such as CO_2 that exert nearly spatially uniform forcing on the climate system (Feldl et al. 2013) and, therefore, do not directly force ITCZ shifts. Rather, these forcing agents cause the planet as a whole to warm and this surface warming has a characteristic hemispheric asymmetry due to the predominance of ocean heat uptake in the Southern Ocean (Armour et al. 2015) in the transient case and the spatial pattern of climate feedbacks in the equilibrium case. From an energetic perspective, global warming can lead to a hemispheric contrast of energy input to the atmosphere (and, thus, an ITCZ shift) by the following mechanisms:

1. Transient ocean heat uptake in one hemisphere which acts as a (temporary) energy sink. For example, heat uptake in the Southern Ocean removes energy from the atmosphere locally and is expected to "pull" southward energy flux across the equator, which is accomplished by a northward ITCZ shift.

2. Shortwave feedbacks that differ between the two hemispheres. For example, sea and land ice has and is projected to decline more rapidly in the NH than the SH resulting in more ASR in the NH through the ice albedo feedback. This leads to a northward ITCZ shift. Additionally, contrasting cloud shortwave feedbacks between the Southern Ocean and Northern Extratropics in simulations of global warming (Zelinka and Hartmann, 2012) have been associated with substantial ITCZ shifts that differ in both direction and magnitude between models (Frierson and Hwang, 2012).

3. Differential surface warming between the two hemispheres leading to energy loss via the emission of longwave radiation. Although the Planck feedback—the change in OLR per unit change in surface temperature-- does differ in magnitude spatially (Soden and Held 2006), the spatial variations are smaller than the mean magnitude of the Planck feedback. Therefore, areas that warm more lose more radiation to space. As a result, the Planck feedback acts as a damping of spatial gradients in temperature which themselves must be sustained by local forcing, feedback processes and/or (up the temperature gradient) energy fluxes in the atmosphere or ocean. Specifically, the preferential surface warming of the NH (Arctic amplification) leads to energy loss from the NH via OLR which, if acting in isolation, would lead to a southward ITCZ shift.

4. Changes in the large scale ocean circulation. The melting of land ice in the NH in a warming planet results in freshwater input to the North Atlantic, which is projected to decrease the AMOC strength by as much as 50% (Swingedouw et al. 2006) resulting in a southward ITCZ shift.

The simulated changes in zonal mean atmospheric heating 150 years after an instantaneous CO_2 quadrupling (hereafter $4XCO_2$) in the CMIP5 multi-model ensemble are shown in Figure 6A. There is significant inter-model spread (differences between the thin dashed lines along the Y-axis) in the energy flux changes. The solid lines show the ensemble average energy flux change and the shaded region indicates the 95% confidence interval of the mean -- the ensemble average change is significantly different from zero where the shaded region does not intercept the x-axis. There are several notable and statistically robust regional changes in both the TOA (red and green) and surface energy fluxes including:

1. Increased energy input to the ocean in Southern ocean where the surface temperature increase is significantly smaller than the global mean in all models. In this region, ocean upwelling associated with Ekman suction by the Westerly surface winds keeps the ocean cool. As a result, the increased downwelling longwave flux associated with greenhouse forcing and, additionally, the warming aloft (due to atmospheric heat transport) exceeds the increase in upward energy flux (primarily latent and sensible heat fluxes) since the sea surface has warmed less than it would in the absence of the upwelling of cold ocean waters (Armour et al. 2015).

2. Increased ocean heat uptake around the NH sea ice edge (60^o N). The loss of sea ice in this region leads the absorption of solar radiation by the ocean surface that would have otherwise been reflected off the ice. This mechanism primarily acts to increase ocean energy input in the summer, whereas the loss of wintertime sea ice leads to ocean energy loss since the ocean is warmer than the local atmosphere in the winter, which results in anomalous upward latent and sensible energy fluxes to the atmosphere if the ocean is open.

3. The increase in both ASR and OLR in the Northern extratropics. Both OLR and ASR increase in response to radiative feedbacks associated with substantial surface warming. ASR increases for two reasons: a. the sea ice and snow on land has melted resulting in a darker surface that reflects less solar radiation and b. the increased moisture content of the atmosphere absorbs more shortwave radiation that would have otherwise been incident on the reflective cloud tops and surface resulting in less SW radiation reflected to space. Changes in solar reflection off of clouds vary drastically between the models and result in inter-model differences in ASR changes. However, the robust increase in ASR can be explained entirely by the robust aforementioned ice albedo and shortwave water vapor feedbacks (Donohoe et al. 2014b) in the absence of any ensemble average cloud feedback. The increase in OLR in the NH is associated with and expected from the increase in surface temperature—which achieves a spatial maxima in the Northern Extratropics—via the Planck feedback.

Despite the above noted robust regional changes in the energy fluxes at the TOA and surface under global warming, even the sign of the change in the hemispheric contrast is ambiguous between the different CMIP5 models. Eight (8) models show an increased energy input into the NH atmosphere and nine (9) models show more energy loss by the NH atmosphere in response to $4XCO_2$. Because the hemispheric contrast of energy input to the atmosphere is equal to the AHT_{EQ} (Equation 3) and – as shown and discussed throughout this chapter—the ITCZ shift is proportional to the change in AHT_{EQ}, there is no robust and consistent ITCZ shift in the ensemble average due to CO_2 forcing. The lack of a consistent change in the hemispheric energy budget is a consequence of the inter-model differences in the hemispheric contrast of TOA radiation changes (σ = 0.14 PW and mean = 0.06 PW) despite the robust ensemble average atmospheric energy loss in the SH associated with ocean heat uptake (mean = 0.12 PW and σ = 0.08). This point can be visualized in Figure 6C where the total change in the hemispheric contrast of atmospheric heating (= AHT_{EQ}) is represented by the colored lines with slope -1 as the sum of the contributions from net radiation at the TOA (abscissa = $\Delta\langle NET_{RAD}\rangle$) and surface energy fluxes (ordinate =Δ <SHF>) via Equation 3. While the models overwhelmingly occupy the upper two quadrants due to a robust increase in <SHF> associated with atmospheric energy loss to the Southern Ocean, the models have wide spread in $\langle NET_{RAD}\rangle$ along the abscissa with no robust ensemble average change. As a result, the total change in AHT_{EQ} spreads across the zero contour (gray line through the origin) with a nearly equal number of models predicting increases in energy input to the NH atmosphere (red contours) as those predicting decreases (blue contours) with the total change being dictated by the simulated change in $\langle NET_{RAD}\rangle$ (dashed purple line).

Why is the change in $\langle NET_{RAD}\rangle$ under global warming ambiguous in sign despite the robust regional changes in ASR and OLR in the Northern Extratropics associated with polar amplification, the ice albedo feedback of melting ice and snow and atmospheric moistening? The net radiative heating of the atmosphere in that region is the difference between the increased

ASR and increased OLR in that region and is, therefore, much smaller in magnitude and less statistically robust than the changes in either ASR or OLR alone (black line in Figure 6C – note the shaded black line intersects the x axis in most regions). We can visualize the compensation between changes in the hemispheric contrast in ASR and OLR by decomposing the total change in $<NET_{RAD}>$ into component contributions from ASR and OLR in Figure 6D. The models distinctly occupy the upper right quadrant due to a robust increase in both ASR ($\Delta<ASR> = 0.29$ PW) and OLR ($\Delta<OLR> = 0.23$ PW) in the NH. However, the changes in <ASR> and <OLR> are positively correlated (dashed purple line) and, thus, the total change on $<NET_{RAD}>$ is ambiguous in sign (models spread across the black, zero contour line into both the red and blues) and dictated primarily by the change in <ASR>.

As has been demonstrated throughout this chapter, meridional shifts in the ITCZ location demand a change in the AHT_{EQ} and, thus, the hemispheric contrast in energy input to the atmosphere. As discussed above, some models simulate increased energy input into the NH due to $4XCO_2$ while a nearly equal number of models simulate more cooling of the NH atmosphere. As a result, the CMIP5 ITCZ shift due to global warming is not significantly different than zero; the ensemble mean ITCZ shift is 0.02° and the inter model spread (2σ) is 0.50°. In the CMIP5 models, inter-model differences in ITCZ location and AHT_{EQ} are well correlated in the pre-industrial simulations (blue circles in Figure 7) and the $4XCO_2$ simulations (red circles) with an approximate relationship of 3° PW^{-1}. Therefore, the inter-model differences in the ITCZ shift and change in AHT_{EQ} are also well correlated ($R = 0.71$) – the changes in the ITCZ/AHT_{EQ} plane are indicated by the black arrows in Figure 7 are primarily along the approximate 3° PW^{-1} regression slope indicated by the purple line. Because the direction of the ITCZ shift and AHT_{EQ} vary widely (the arrows point in different directions), the ensemble average changes (dark black arrow) are small and not significantly different from zero. The essential point is that any ITCZ shift must be accompanied by a change in the hemispheric energy budget of the atmosphere and (despite several prominent regional energetic changes) the uncertainties in the projected changes to the hemispheric contrast of atmospheric heating due to global warming are larger than any projected changes.

Therefore, it is unclear if we should expect the ITCZ to shift northward or southward under global warming. However, the approximate quantitative relationship between the ITCZ location and the hemispheric contrast of atmospheric heating (~3° PW^{-1}) -- which seems to capture past changes ITCZ shifts on timescales ranging from the seasonal cycle, to the inter-annual variability to the shift due to external forcing -- suggests that ITCZ shifts will be small in the annual zonal mean (<1°). Larger magnitude shifts would demand substantial changes in the large scale energy budget of the climate system which are unrealized in climate models, even under extreme forcing such as CO_2 quadrupling and the forcing of the Last Glacial Maximum.

Citations.

Arbuszewski, J., P. deMenocal, C. Clroux, L. Bradtmiller, and A. Mix, 2013: Meridional shifts of the Atlantic intertropical convergence zone since the last glacial maximum. J. Atmos. Sci., 6, 959962.

Armour, K.C., J. Marshall, J. Scott, A. Donohoe and E.R. Newsom, 2015: The Southern Ocean thermostat. Submitted to Nat. Geosci.

Allen, R., S. Sherwood, J. Norris, and C. Zender, 2012: Recent northern hemisphere tropical expansion primarily driven by black carbon and tropospheric ozone. Nature, 485, 350–354.

Bowman, K.P. and P.J. Cohen, 1997: Interhemispheric exchange by seasonal modulation of the Hadley circulation, J. Atmos. Sci., 54, 2045-2059.

Ceppi, P., T.-T. Hwang, X. Liu, D.M.W. Frierson and D.L. Hartmann, 2013: The relationship between the ITCZ and the Southern Hemispheric eddy-driven jet. J. Geophys. Res. Atmos., 118, 5136-5146.

Chiang, J. and C. Bitz, 2005: The influence of high latitude ice on the position of the marine intertropical convergence zone. Climate Dyn., DOI 10.1007/s00 382–005–0040–5.

deMenocal, P. *et al., 2000:* Abrupt onset and termination of the African Humid Period: rapid climate responses to gradual insolation forcing. Quat. Sci. Rev. 19, 347–361

Donohoe, A. and D. Battisti, 2011: Atmospheric and surface contributions to planetary albedo. J. Climate, 24 (16), 4401–4417.

Donohoe, A., D. Frierson, and D. Battisti, 2013a: The effect of ocean mixed layer depth on climate in slab ocean aquaplanet experiments. Climate Dyn., 26, 15 Pages, doi:10.1007/s00382-013-1843-4.

Donohoe, A., J. Marshall, D. Ferreira, and D. McGee, 2013b: The relationship between itcz location and atmospheric heat transport across the equator: from the seasonal cycle to the last glacial maximum. J. Climate, 26 (11), 3597–3618.

Donohoe, A. and D. Battisti, 2014: The seasonal cycle of atmospheric heating and temperature. J. Climate, 26 (14), 4962–4980.

Donohoe, A., J. Marshall, D. Ferreira, K. Armour, and D. McGee, 2014: The inter-annual variability of tropical precipitation and inter-hemispheric energy transport. J. Climate, 27 (9), 3377–3392.

Donohoe, A., K.C. Armour, A.G. Pendergrass and D.S. Battisti, 2014. Shortwave and longwave contributions to global warming under increasing CO_2. PNAS, November 10, 2014. doi:10.1073/pnas.141219.

Dwyer, J., M. Biasutti, and A. Sobel, 2012: Projected changes in the seasonal cycle of surface temperature. J. Climate, 25, 6359–6374.

Feldl, N., D.M.W. Frierson, and G.H. Roe, 2014: The influence of regional feedbacks on circulation sensitivity. Geophys. Res. Lett., 41, doi:10.1002/2014GL059336.

Frierson, D. M. W. and Y.-T. Hwang, 2012: Extratropical influence on itcz shifts in slab ocean simulations of global warming. J. Climate, 25, 720–733.

Frierson, D., Y.T. Hwang, N.S. Fuckar, R. Seager, S.M. Kang, A. Donohoe, E. Maroon, X. Liu and, D.S. Battisti 2013: Why does tropical rainfall peak in the northern hemisphere? the role of the oceans meridional overturning circulation. Nature Geosci., 6, 940–944.

Hadley, G., 1735: Concerning the cause of the general tradewinds. Philos. Trans. Roy. Soc, 29, 58–62.

Haug, G., K. Hughen, D. Sigman, L. Peterson, and U. Rohl, 2001: Southward migration of the intertropical convergence zone through the holocene. Science, 293, 1304–1308.

He, F., Z. Liu, O. Bette, P. Clark, A. Carlson, and E. Brady, 2010: North atlantic melting water forcing of early deglacial warming in the southern ocean and two-step north pacific ventilation: A transient gcm study with ccsm3.

Heaviside, C. and A. Czaja, 2013: Deconstructing the hadley cell heat transport. Quart. J. Roy. Meteor. Soc., 139 (677), 2181–2189.

Held, I., 1980: Nonlinear axially symmetric circulations in a nearly inviscid atmosphere. J. Atmos. Sci., 37, 515–533.

Held, I., 2001: The partitioning of the poleward energy transport between the tropical ocean and atmosphere. J. Atmos. Sci., 58, 943–948.

Hwang, Y. and D. Frierson, 2013: Link between the double-intertropical convergence zone problem and cloud bias over southern ocean. 110, 4935–4940.

Hwang, Y.-T., Frierson, D. M. W. and S. M. Kang, 2013. Anthropogenic sulfate aerosol and the southward shift of tropical precipitation in the 20th century. Geophys. Res. Lett., 40, 1-6, doi: 10.1002/grl50502, 2013

Johanson, C. and Q. Fu, 2009: Hadley cell widening: model simulations versus observations. J. Climate, 22, 2713–2725.

Kalnay, E., et al., 1996: The NCEP/NCAR 40-year reanalysis project. Bull. Amer. Meteor. Soc.

Kang, S., R. Seager, D. Frierson, and X. Liu, 2014: Croll revisited: Why is the northern hemisphere warmer than the southern hemisphere? Climate Dyn., 16, doi:10.1007/s00382-014-2147-z.

Kato, S., N. Loeb, P. Minnis, J. Francis, T. Charlock, D. Rutan, E. Clothiaux, and S. Sun-Mack, 2006: Seasonal and interannual variations of top-of-atmosphere irradiance and cloud cover over polar regions derived from ceres data set. Geophys. Res. Lett., 33, doi:10.1029/2006GL026 685.

Koppen, W., 1936: Das geographisca System der Klimate, in: Handbuch der Klimatologie, edited by: Koppen, W. and Geiger, G., 1. C. Gebr, Borntraeger, 1–44.

Liu, Z., B. Otto-Bliesner, F. He, E. Brady, R. Tomas, P. Clark, and A. Carlson, 2009: Transient simulation of last deglaciation with a new mechanism for bølling-allerød warming. Science, 325 (5938), 310–314.

Lindzen, R.S. and A.Y. Hou, 1988: Hadley circulations of zonally averaged heating centered off the equator. J. Atmos. Sci., 45, 2416-2427.

Marshall, J., A. Donohoe, D. Ferreira, and D. McGee, 2013: The oceans role in setting the mean position of the inter-tropical convergence zone. Climate Dyn., 14.

Meehl, G. A., C. Covey, T. Delworth, M. Latif, B. McAvaney, J. F. B. Mitchell, R. J. Stouffer, and K. E. Taylor, 2007: The WCRP CMIP3 multi-model dataset: A new era in climate change research. Bull. Amer. Meteor. Soc., 88, 1383–1394.

Merlis, T. M., M. Zhao, and I.M. Held, 2013: The sensitivity of hurricane frequency to ITCZ changes and radiatively forced warming in aquaplanet simulations. Geophysical Research Letters, 40, 4109-4114.

Adam,O. T. Bischoff, and T. Schneider, 2015. Seasonal and interannual variations of the energy flux equator and ITCZ. Part I: Zonally averaged ITCZ position. In Review. Journal of Climate.

Peltier, W., 2004: Global glacial isostasy and the surface of the ice-age earth: The ice-5g (vm2) model and grace. Annu. Rev. Earth Planet. Sci., 22, 111–149.

Peterson, L., G. Haug, K. Hughen, and U. Rohl, 2000: Rapid changes in the hydrologic cycle of the tropical atlantic during the last glacial. Science, 290, 1947–1951.

Sachs, J., D. Sachse, R. Smittenberg, Z. Zhang, D. Battisti, and S. Golubic, 2009: Southward movement of the pacific intertropical convergence zone ad 1400-1850. natgeo, 2, 519–525.

Schneider, T., T. Bischoff, and G. Haug, 2014: Migrations and dynamics of the intertropical convergence zone. Nature, 513, 45–53.

Soden, B. and I. Held, 2006: An assessment of climate feedbacks in coupled ocean-atmosphere models. J. Climate, 19, 3354–3360.

Swingedouw, D., P. Braconnot, and O. Marti, 2006: Sensitivity of the Atlantic Meridional Overturning Circulation to the melting from northern glaciers in climate change experiments. Geophys. Res. Lett., 33, L07711, doi:10.1029/2006GL025765.

Sivakumar, M.V.K., H.P. Das, and O. Brunini, 2005: Impacts of present and future climate variability and change on agriculture and forestry in the arid and semi-arid tropics**.** Clim. Chang., 70, 31-72.

Vimont, D. J., and J. P. Kossin, 2007: The Atlantic Meridional Mode and hurricane activity, Geophys. Res. Lett., 34, L07709.

Voigt, A., S. Bony, J. Dufresne, and B. Stevens, 2014: The radiative impact of clouds on the shift of the intertropical convergence zone. Geophys. Res. Lett., 41 (12), 4308–4315.

Voigt, A., B. Stevens, J. Bader, and T. Mauritsen, 2013: The observed hemispheric symmetry in reflected shortwave irradiance. J. Climate, 26, 468–477

Xie, P. and P. Arkin, 1996: Analyses of global monthly precipitation using gauge observations, satellite estimates, and numerical model predictions. J. Climate, 9, 840–858.

Zelinka, M. and D. Hartmann, 2012: Climate feedbacks, and their implications for poleward energy flux changes in a warming climate. J. Climate, 25, 608-624.

Figures Captions.

Figure 1. (Right panels) The colors show the climatological precipitation from the NOAA merged analysis (Xie and Arkin, 1996) and blue lines denote the latitude of maximum precipitation at each longitude. (Left Panels) The purple line is the zonal mean precipitation and the colors show the mass overturning streamfunction in Sverdrups from the NCEP reanalysis (Kalnay et al. 1996). The stream function is defined as positive (red) when the circulation is clockwise and negative (blue) when the circulation is counter-clockwise. The vertically and zonally integrated atmospheric energy transport at the equator (AHT_{EQ}) is denoted by the green arrow. The top panel shows the annual mean, the middle panel is June and the bottom panel shows January.

Figure 2. (A) Cartoon of the relationship between ITCZ location, the Hadley cell, AHT_{EQ} and the terms in the hemispheric energy budget of the atmosphere. (B) Observational estimates of the terms in the annual mean hemispheric energy budget. Values are derived in Marshall, et al. (2013) and Frierson et al. (2013).

Figure 3. The relationship between ITCZ location and the atmospheric energy transport across the equator spanning different timescales in observations, models, and paleoclimate reconstructions. In all cases, the centroid of tropical precipitation (P_{CENT}) is used as a metric for the ITCZ location. Although the domain and range differs substantially between the panels, the relative scaling of the axes is constant throughout the panels .(A) Annual mean climatology in (red crosses) coupled CMIP3 pre-industrial simulations and (blue box) observational estimates with uncertainty (1σ) indicated by the dashed blue rectangle (Marshall et al. 2013). (B) Observed seasonal cycle (Donohoe et al. 2013). Monthly means are the blue crosses and the thick dashed blue line represents the linear best fit with length equal to the amplitude (first harmonic) of the seasonal cycle. Each of the dashed lines represents the slope and amplitude of a

CMIP3 model with the color representing the slope value as given by the colorbar inset in the figure. (C) Observed interannual variability (Donohoe et al. 2014) of the ITCZ (from NOAA CPC merged analysis) and AHT_{EQ} (from NCEP reanalysis). The colors are the smoothed probability distribution function of monthly anomalies, the crosses are the annual data (low pass filtered with cutoff period of 1 year) and the dashed line is the linear best fit. (D) Response to anthropogenic and paleoclimate forcing (Donohoe et al. 2014) alongside proxy estimates based on sea surface temperature reconstructions (Mcgee et al. 2014). Each cross is a different simulation, color coded by experiment type (red=$2XCO_2$, blue = LGM and green=mid-Holocene) and the solid squares and shaded areas represent the ensemble average and one standard deviation. Circles and dashed crosses are the paleo estimates and uncertainity.

Figure 4. (Top Panel) Time series of 10 year low pass filtered (red) ITCZ location (as measured by P_{CENT}) and (blue) AHT_{EQ} in the CCSM3 transient climate evolution (TraCE) experiment. The AHT_{EQ} has been negated and scaled by a factor of 3 as shown on the y-axis to the right. The vertical shading shows the time periods used to define the (blue) LGM, (gray) Heinrich Stadial 1 and (green) mid-Holocene. (Middle Panel) The partitioning of AHT_{EQ} into (green) surface and radiative (orange) heating of the NH via Equations 3 and 4). The AHT_{EQ} has been negated (right y-axis) so that the positive axis corresponds to radiative heating of the NH and a northward ITCZ shift. (Bottom Panel) The contours show smoothed probability distribution functions in the $AHT_{EQ}/ITCZ_{LOC}$ plane for the (blue) LGM, (gray) Heinrich Stadial 1, (green) mid-Holocene and (red) modern. Annual mean values are shown with small circles. The dashed black line shows the linear best fit to all the data which falls on the seasonal best fit.

Figure 5. (Top panels) Annual mean and (bottom panels) NH summer mass overturning streamfunction (gray contours) and precipitation (blue lines) for the (left panels) 50 meter and (right panels) 2.4 meter slab ocean aquaplanet simulations. The orange line is the energy input to the atmosphere--defined as the shortwave absorption in the atmospheric column plus the upward turbulent and longwave flux at the surface—with annual mean shown in the top panels and the seasonal anomaly shown in the lower panels. The mass overturning streamfunction is shown in gray contours with solid lines denoting clockwise rotation and dashed line denoting counter-clockwise rotation. The contour interval is 20 Sv (10^9 kg s^{-1}) for the top panels and 50 Sv for the bottom panels.

Figure 6. (A) The zonal mean change in energy input to the atmosphere in the $4XCO_2$ CMIP5 simulations. ASR is shown in red, OLR in green and the surface energy flux in blue. The dashed lines are the individual models, the solid line is the ensemble mean and the shaded region is the 95% confidence interval of the ensemble mean. (B) As in (A) except the hemispheric contrast of the energy flux change (half the difference between the NH and SH) with total change in energy input to the atmosphere in black. (C) The spatially integrated hemispheric contrast of energy input to the NH atmosphere by SHF (abscissa) and TOA radiation (ordinate). The total change in energy input is the sum of the abscissa and ordinate and is indicated by the diagonal colored contours with slope negative unity. The zero contour is gray. The open circles are individual models and the solid circle is the ensemble mean. The dashed purple line is the linear best fit. (D) As in (C) but for the decomposition of the change in the hemispheric contrast of TOA radiation into ASR and OLR components. In this case, the total TOA change is the difference between ASR and OLR and is indicated by the slanted color lines with positive unity slope.

Figure 7. Scatter plot of ITCZ position (ordinate) and AHT_{EQ} in the CMIP5 simulations. The blue dots show the pre-industrial simulation in individual models and the red dots are for the $4XCO_2$ simulations. The arrows indicate the change due to global warming. The ensemble average is shown by the shaded squares and the purple line is the linear best fit to all simulations.

A

ANNUAL

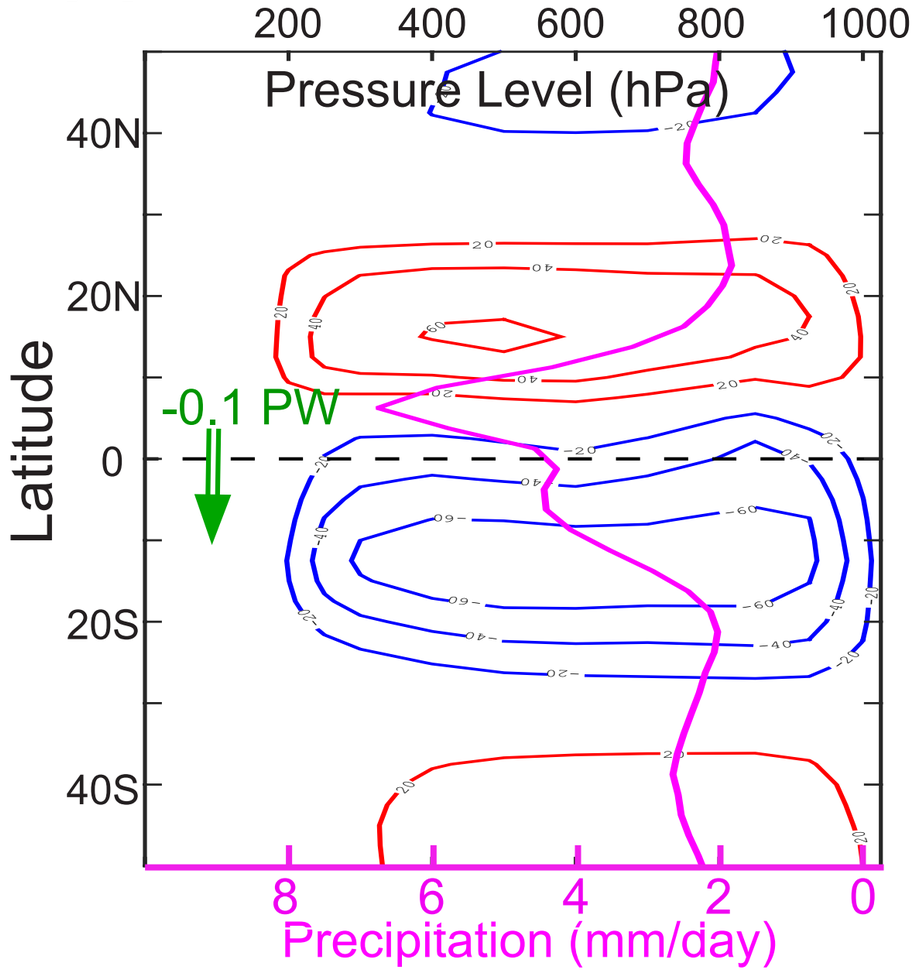

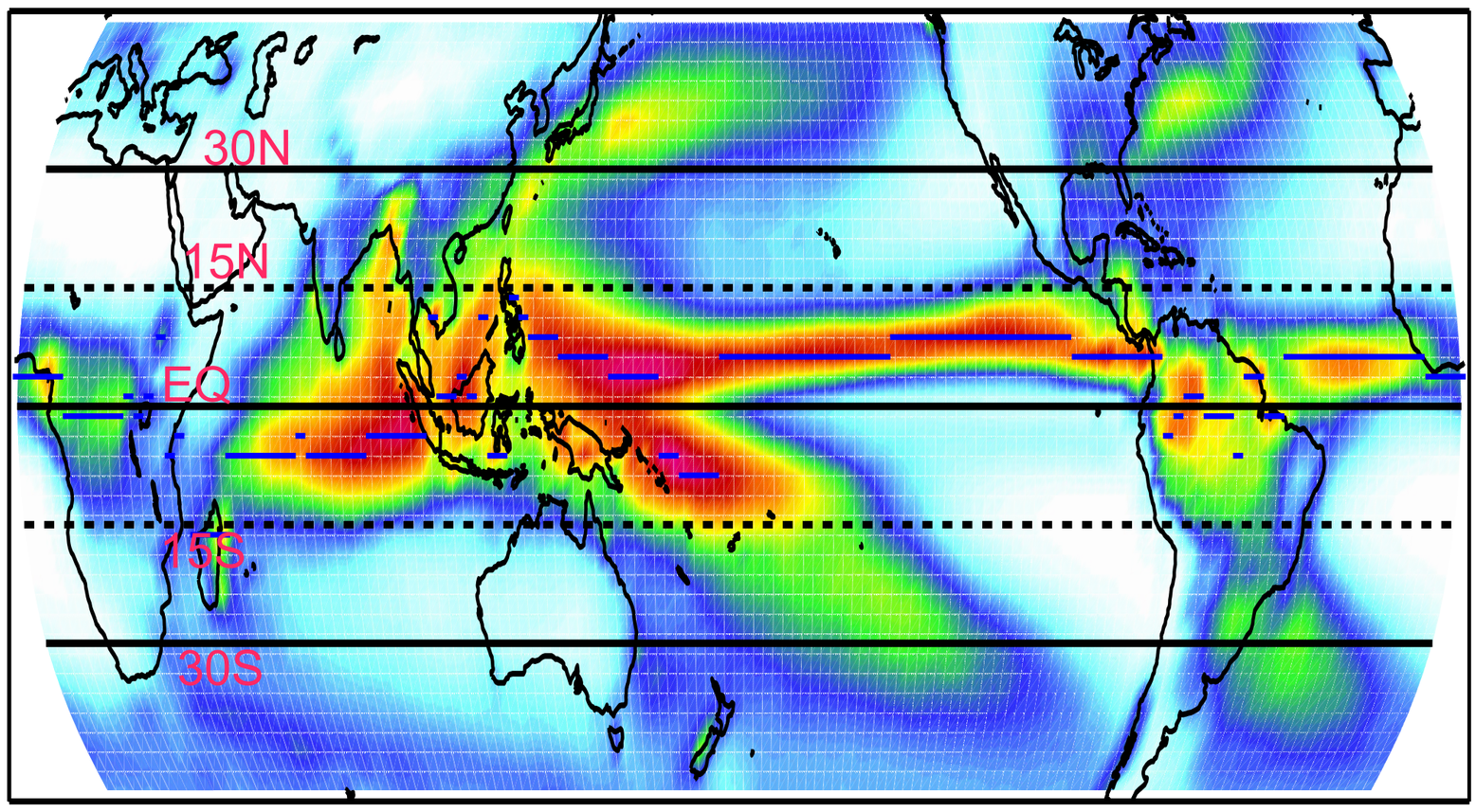

Mass overturning streamfunction (Sverdrups)

Atmospheric Heat Transport (PW)

Precipitation (mm/day)

2 4 6 8 10 12

Latitude of max precip.

B

JUNE

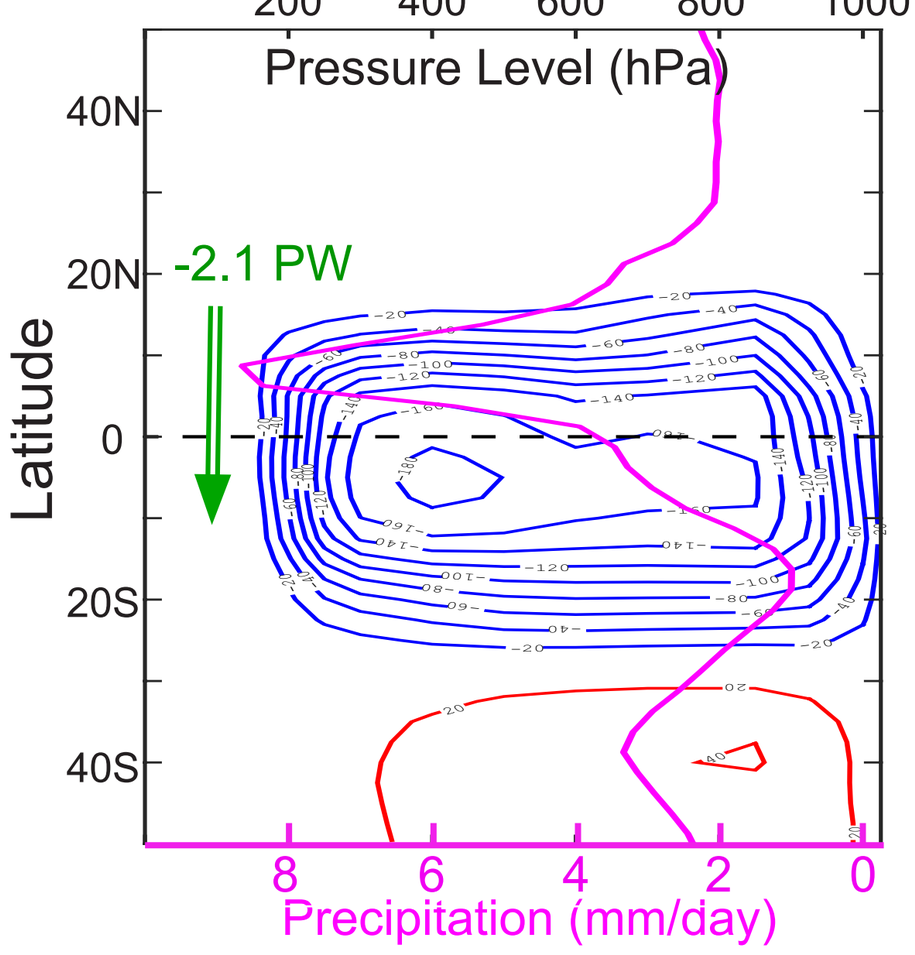

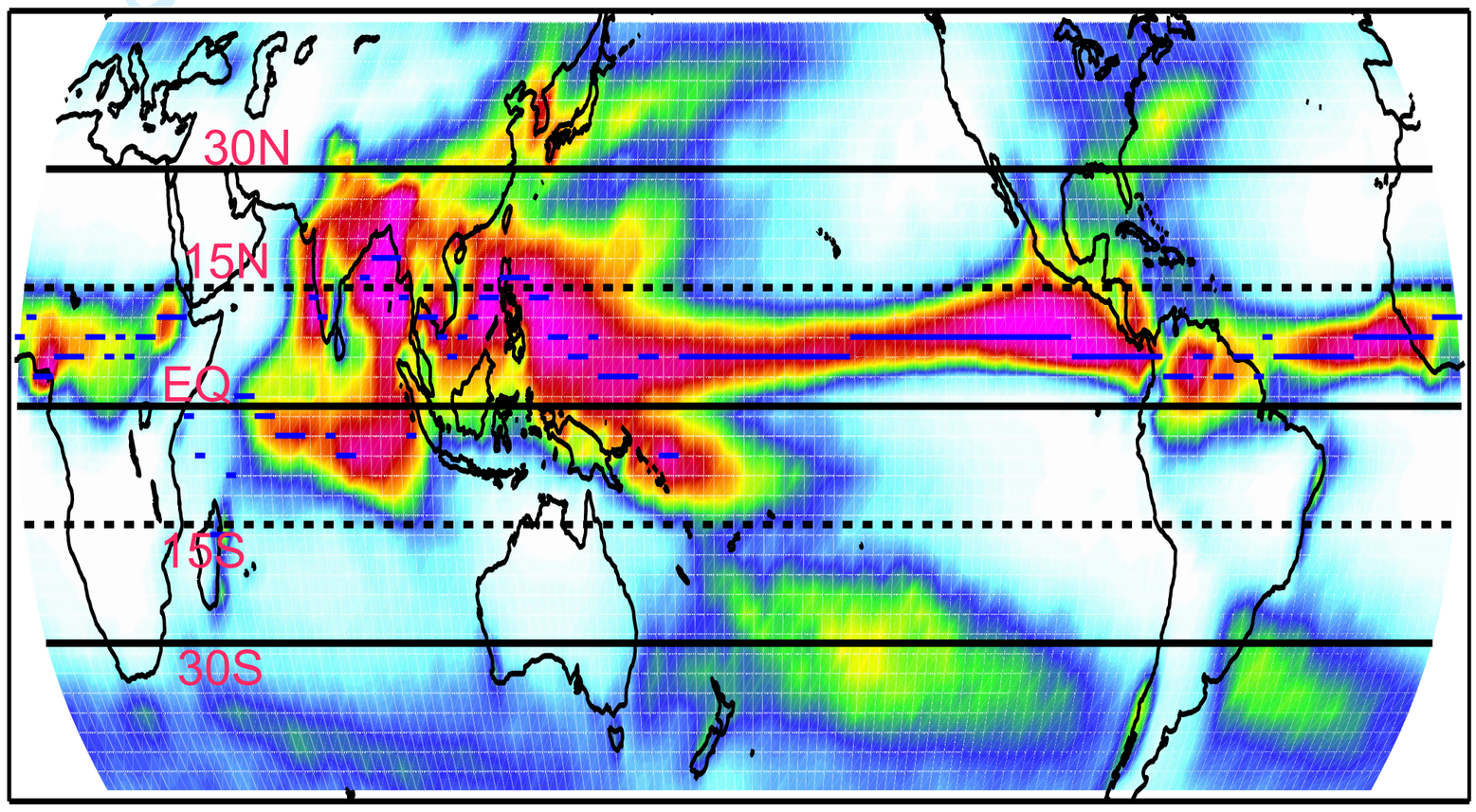

C

JANUARY

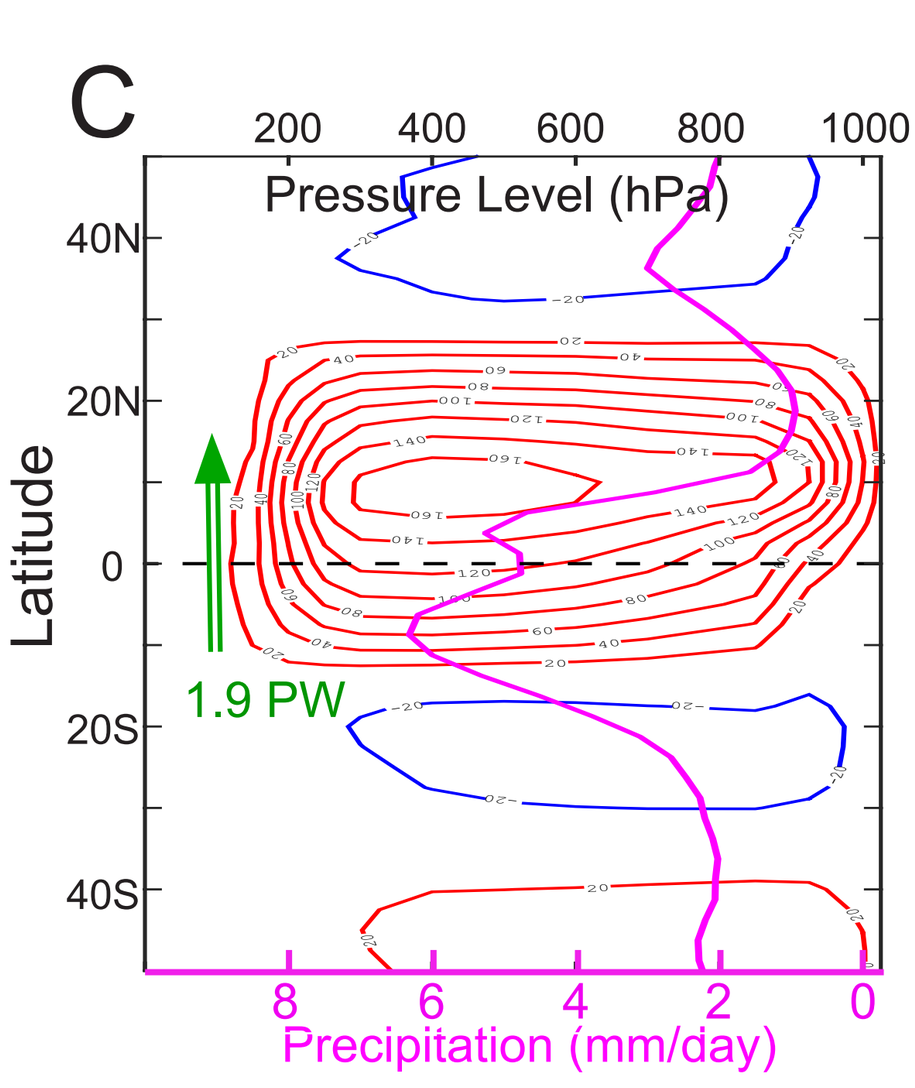

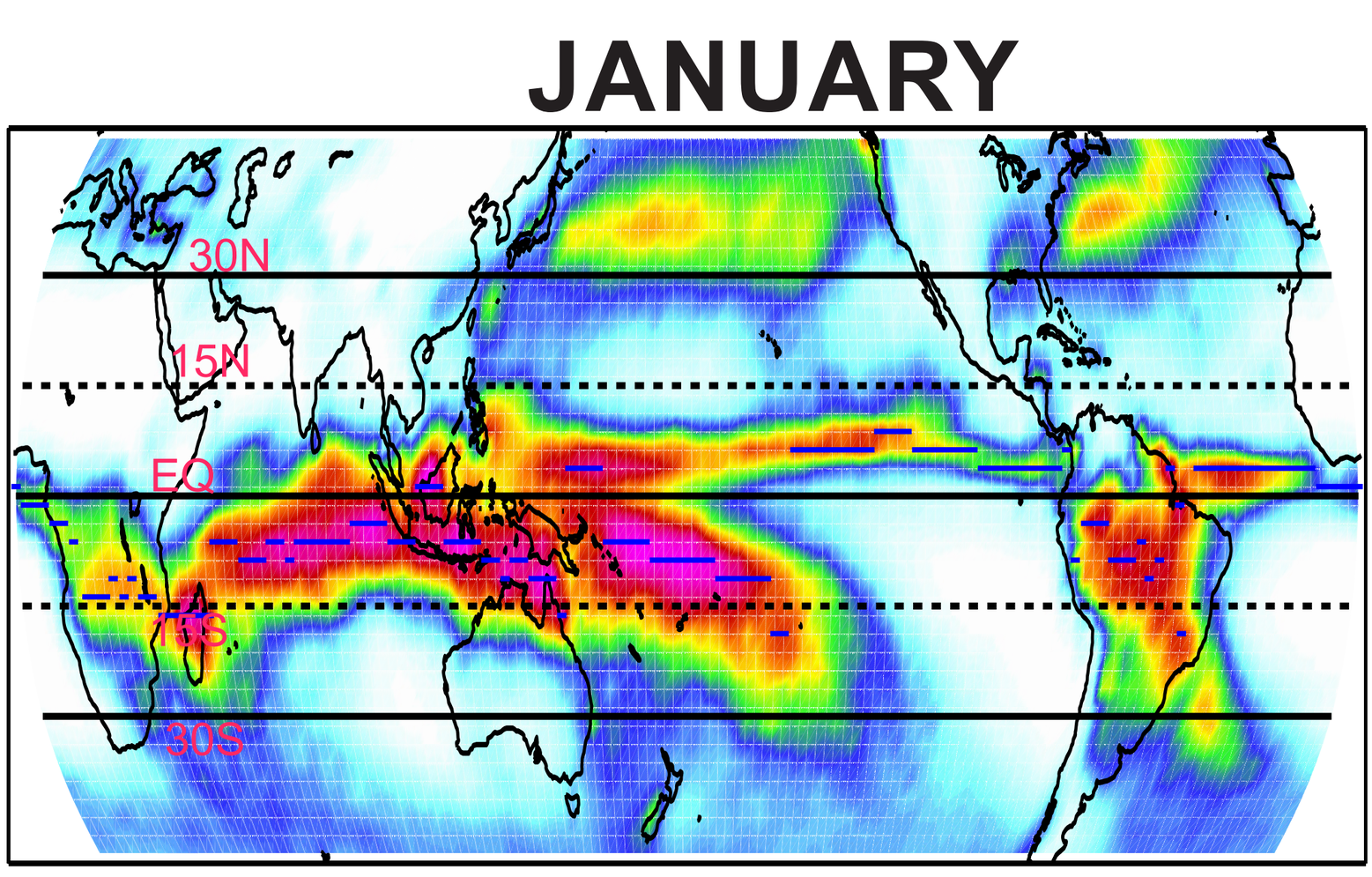

A Schematic of relationship between ITCZ location and AHT_{EQ}

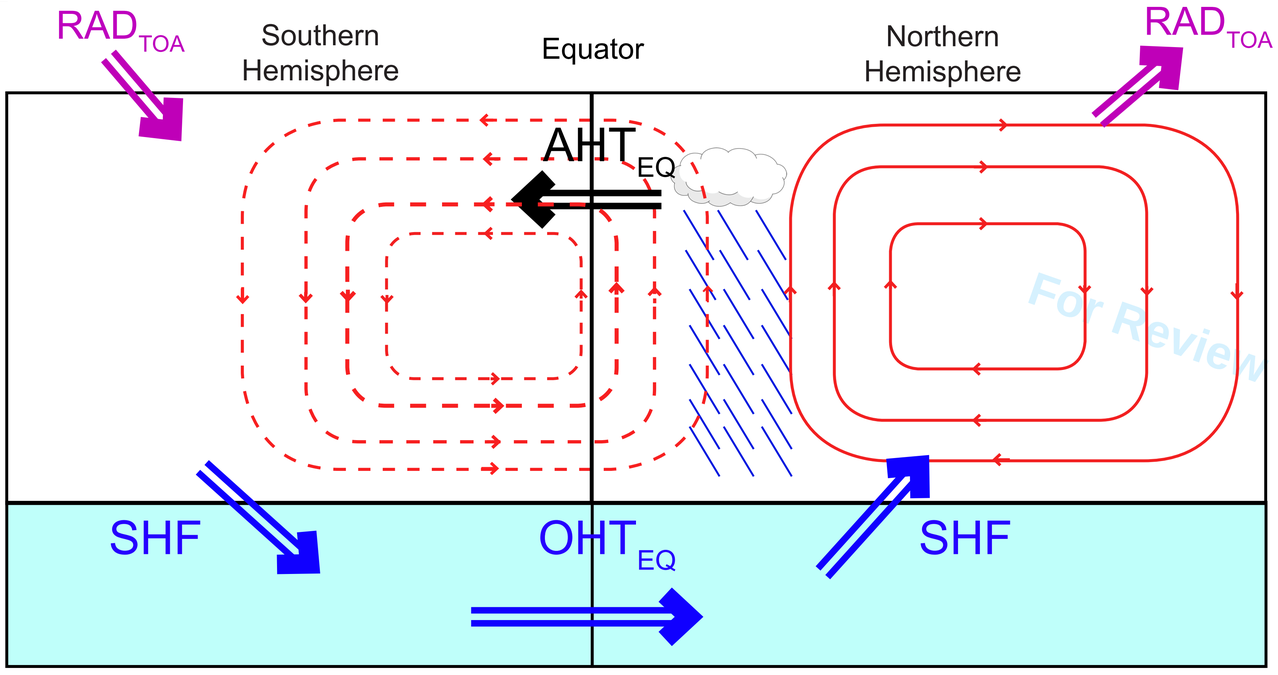

Mass overturning streamfunction

B Observed Hemispheric Energy Budget

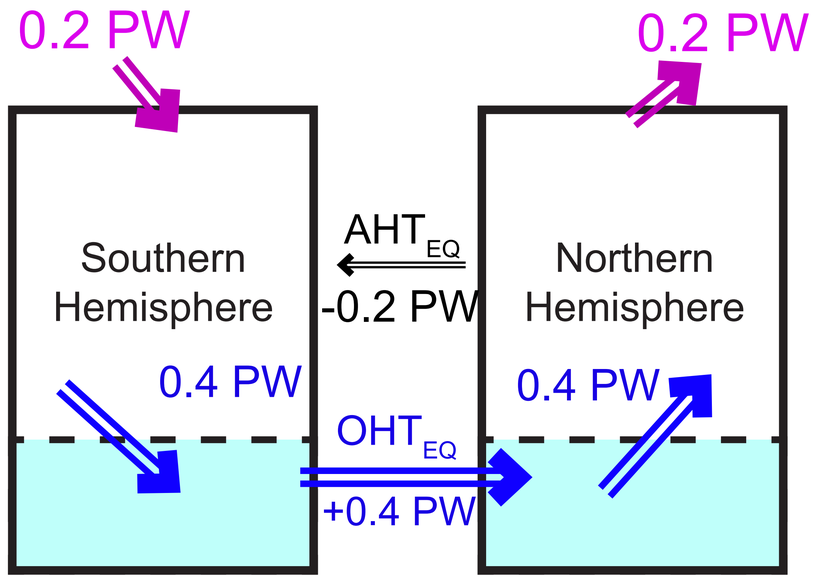

↘ Atmospheric Heat Transport (AHT_{EQ})

↘ Ocean Heat Transport (OHT_{EQ})

↘ Net radiation at TOA

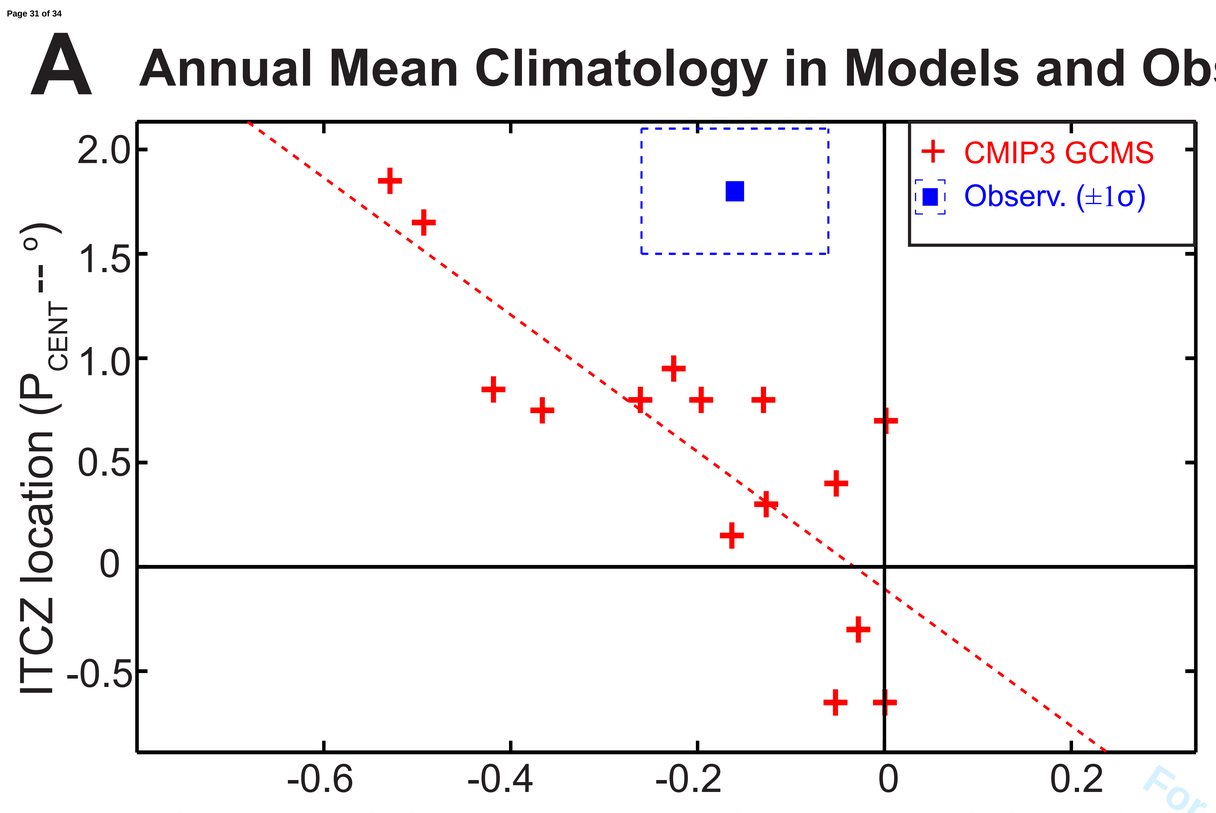

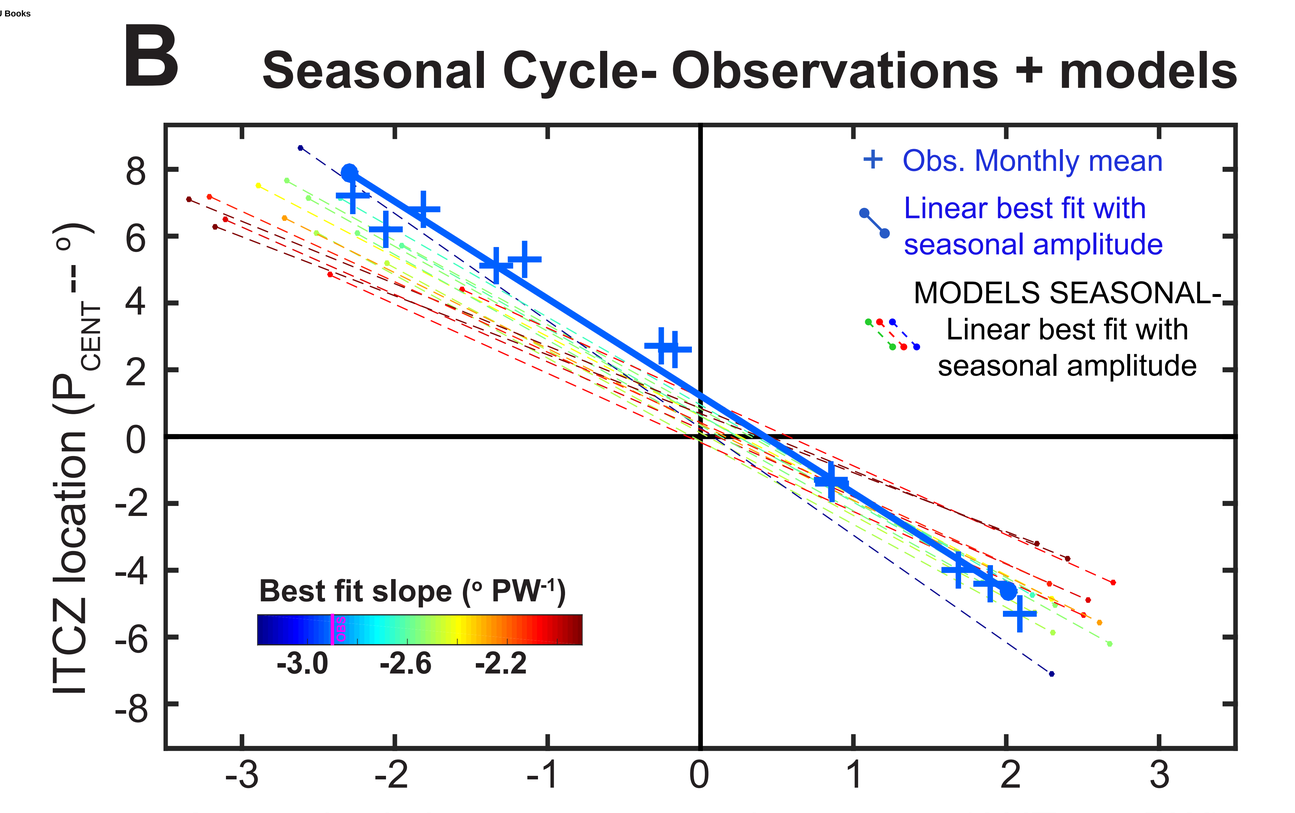

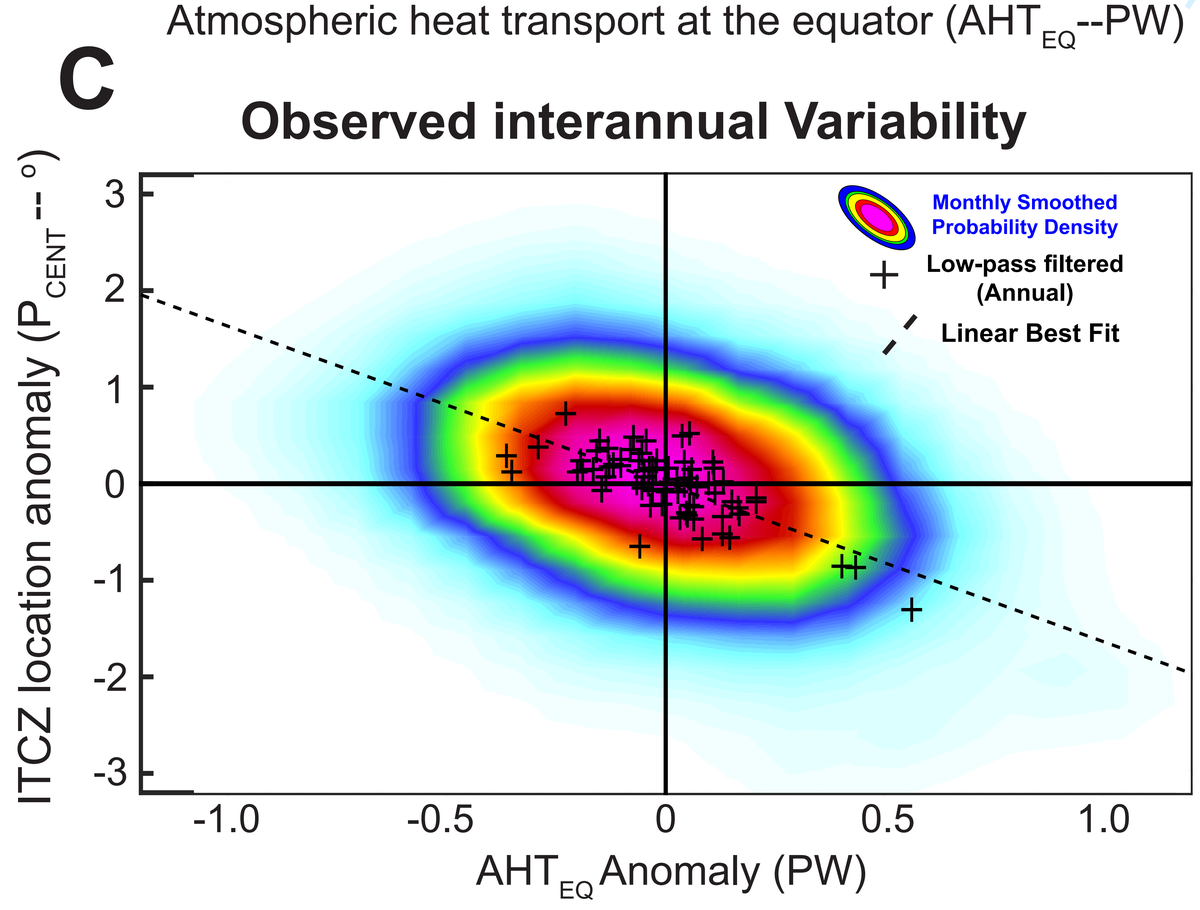

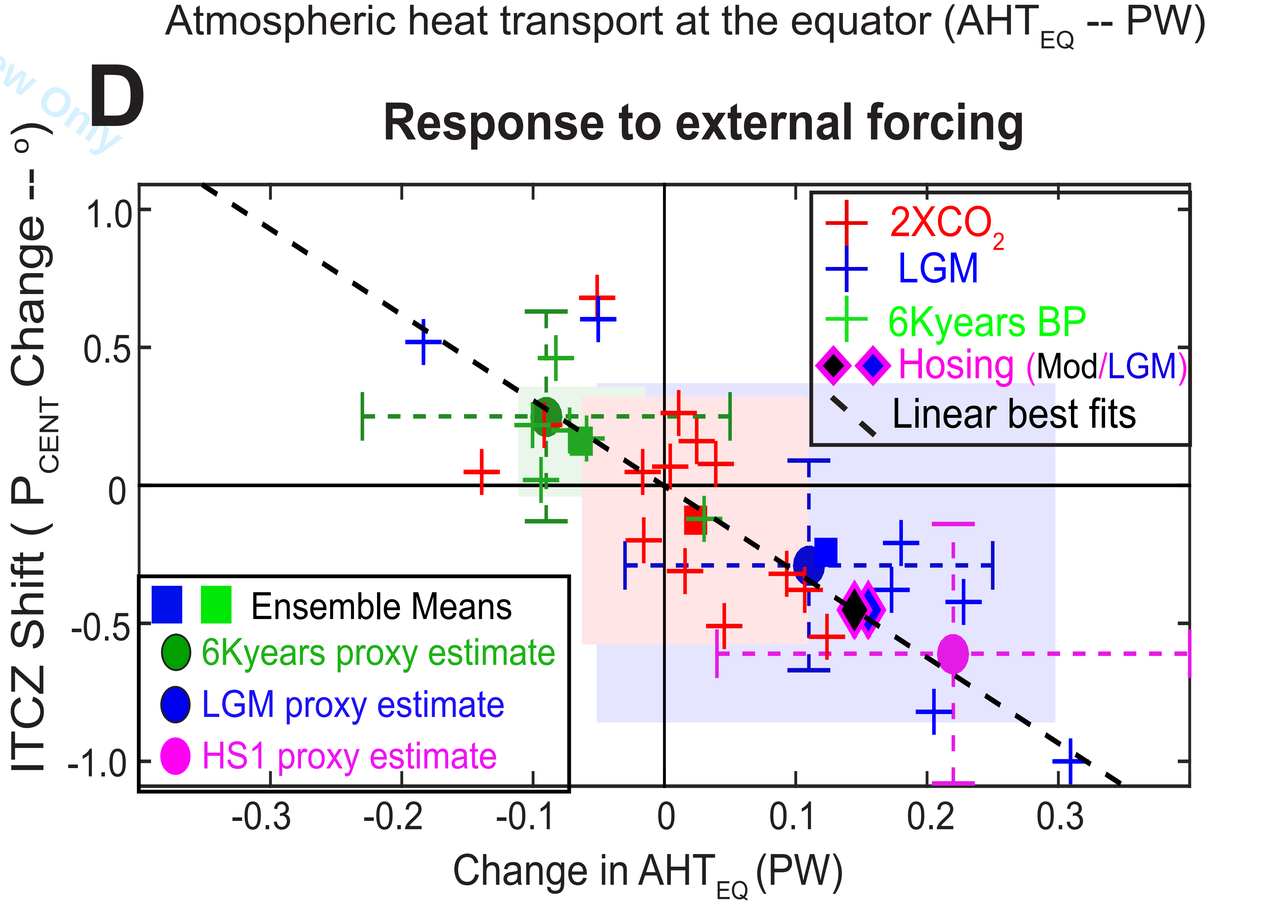

TRACE Experiment ITCZ location and AHT_{EQ}

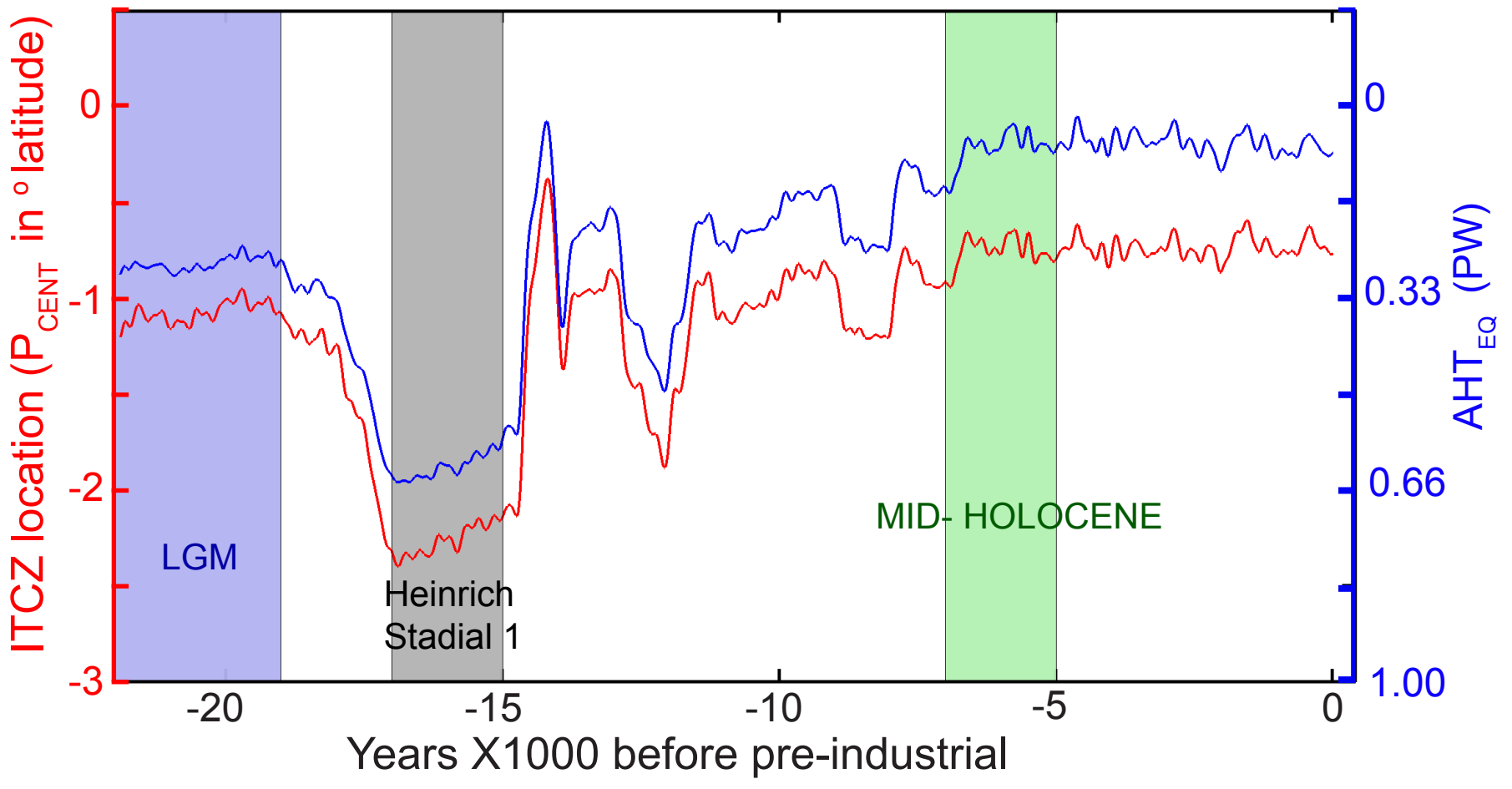

AHT_{EQ} decomposed into hemispheric asymmetries in surface and radiative fluxes

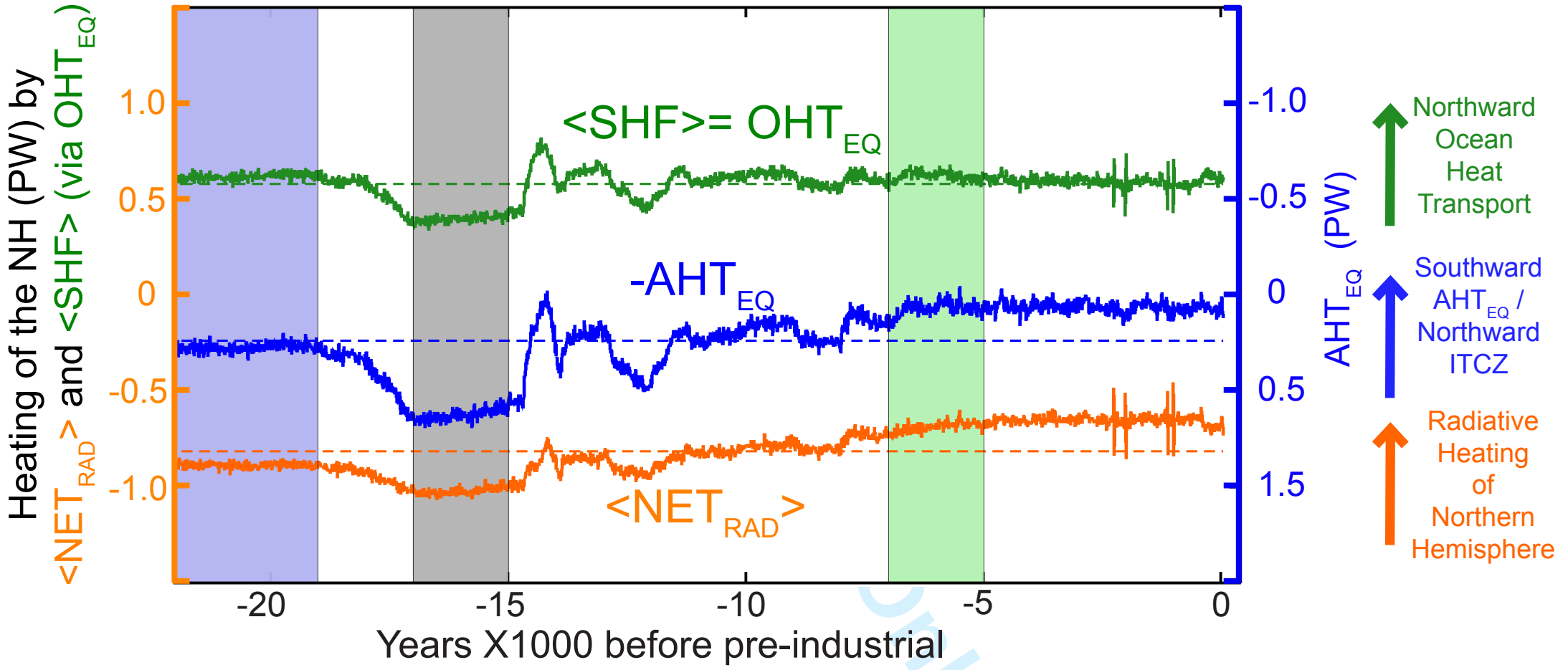

Seasonal Histograms of ITCZ and AHT_{EQ} for LGM, Heinrich 1, Mid-Holocene and Modern

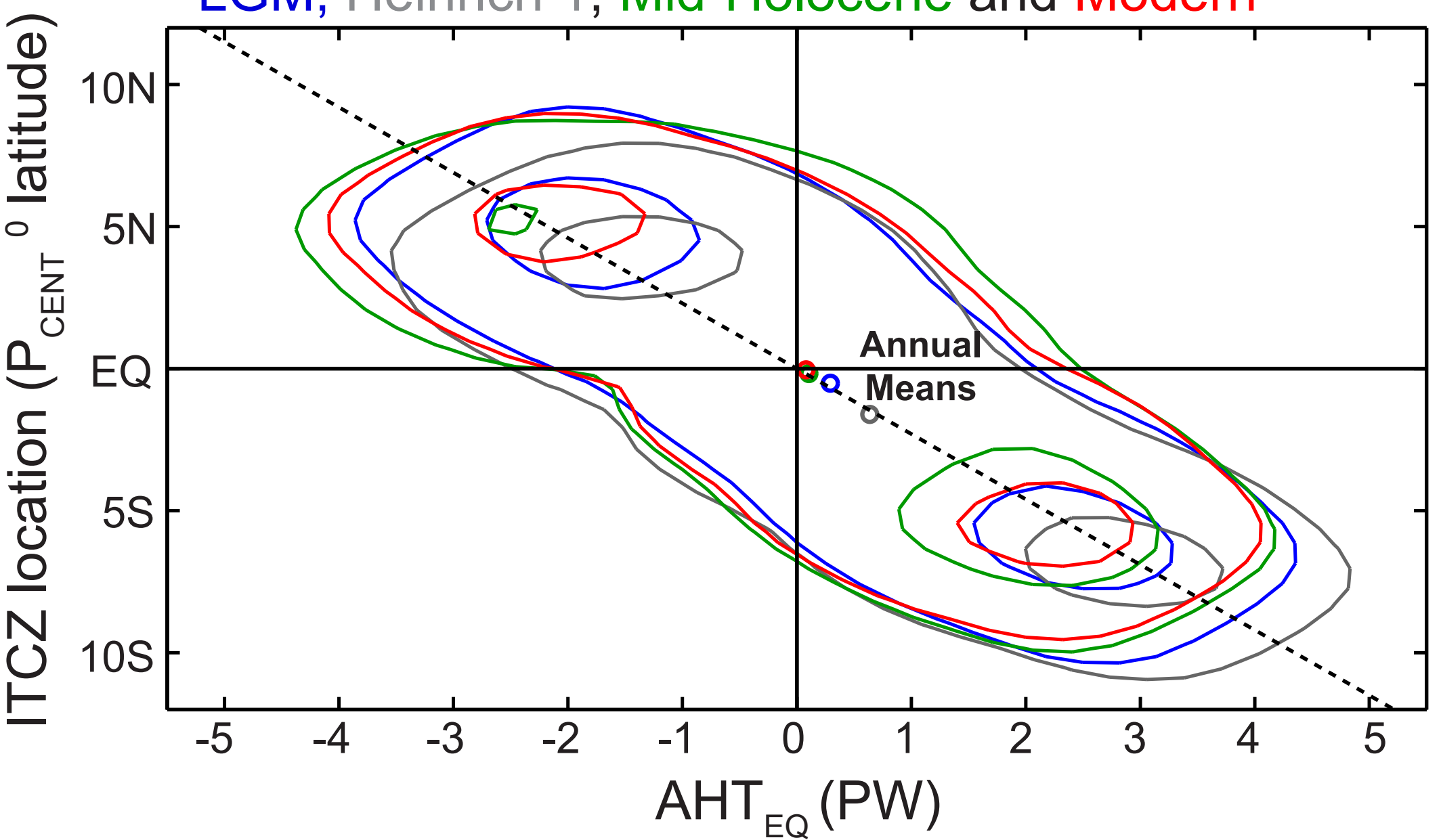

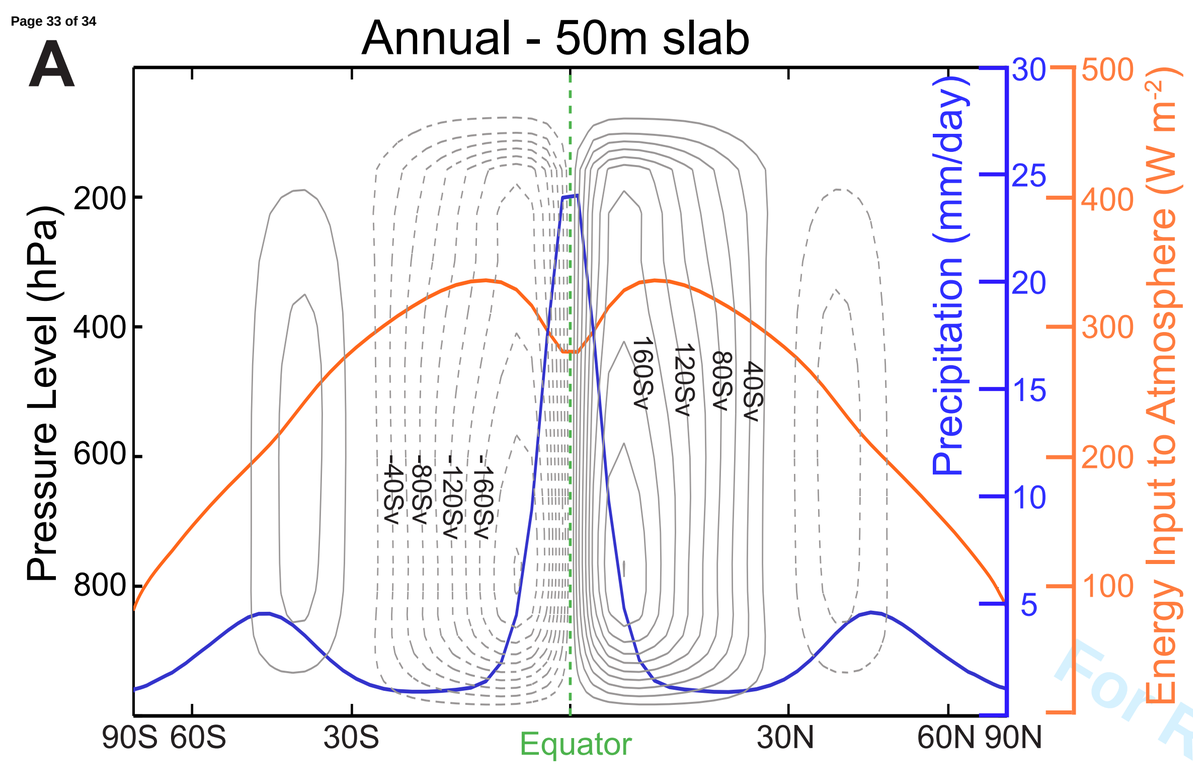

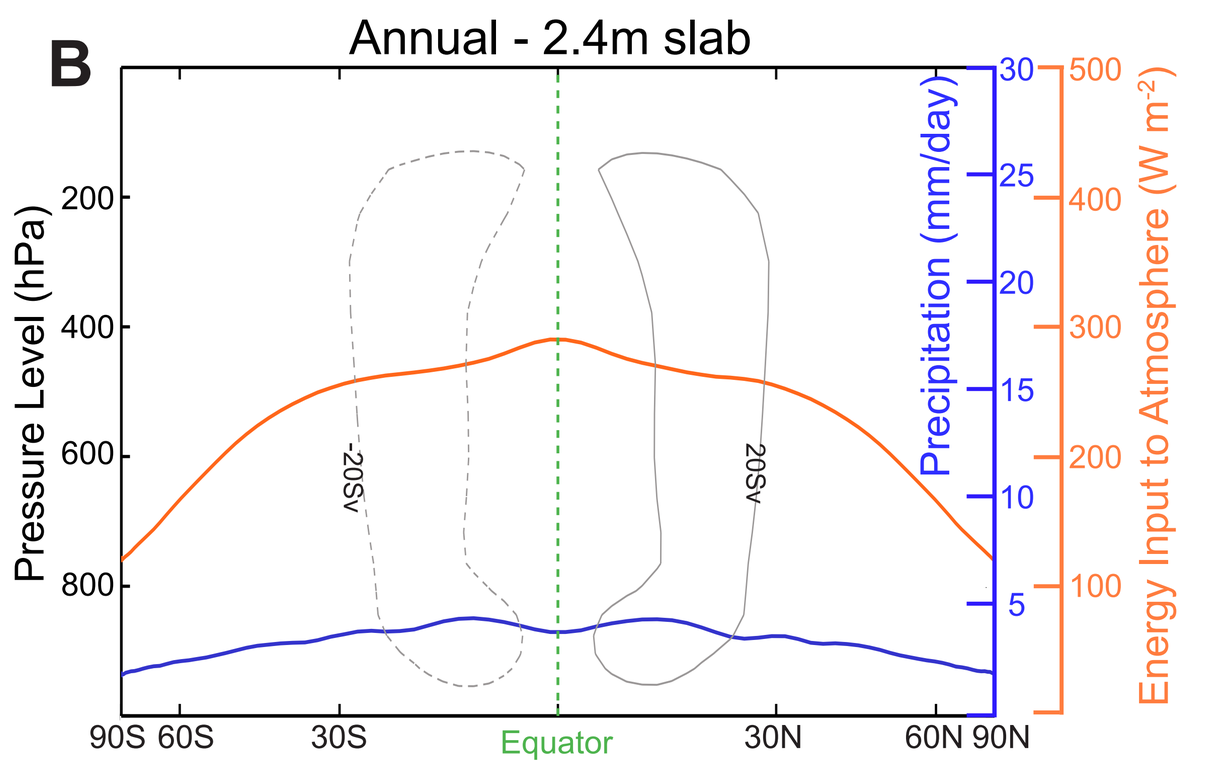

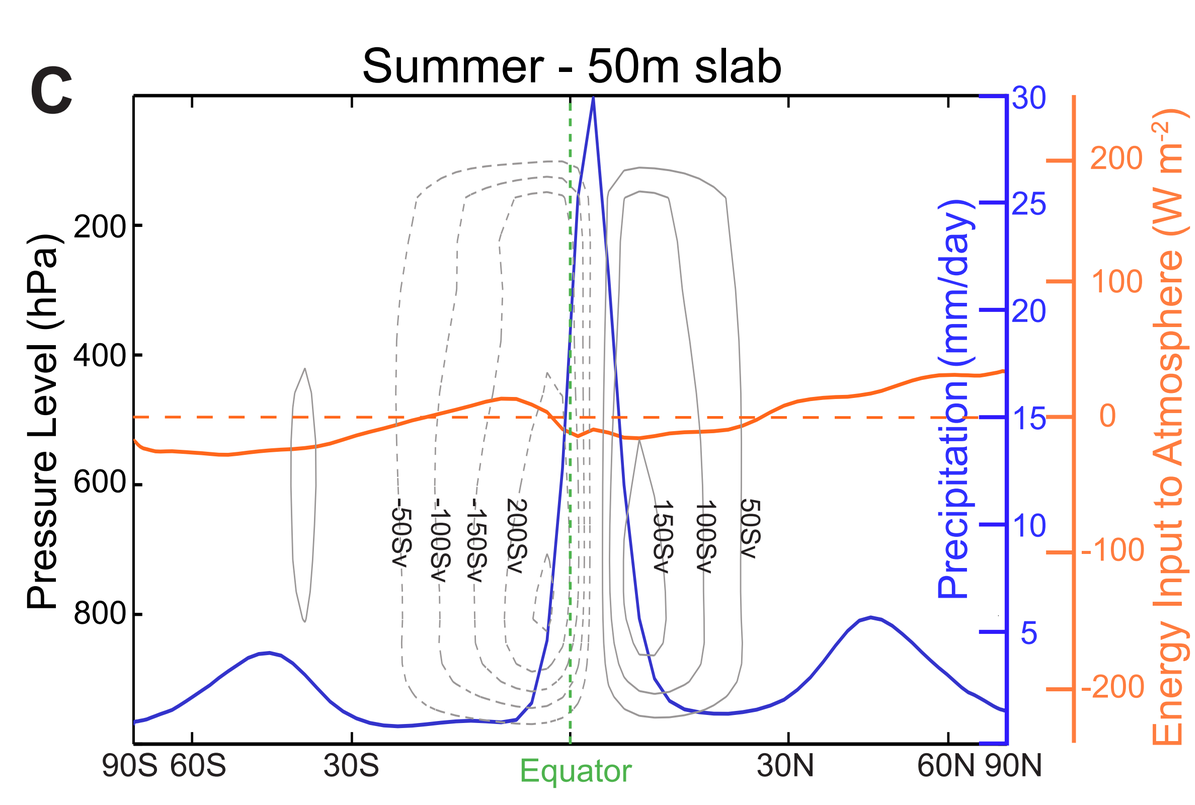

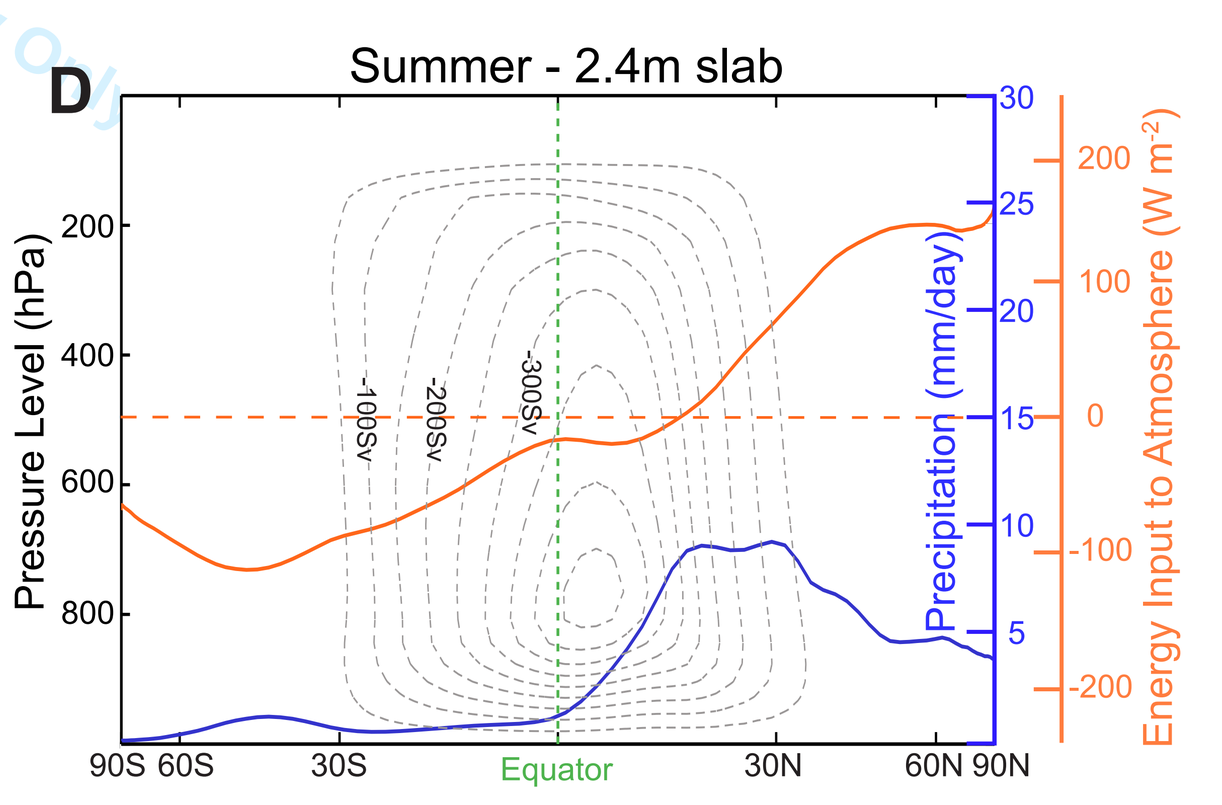

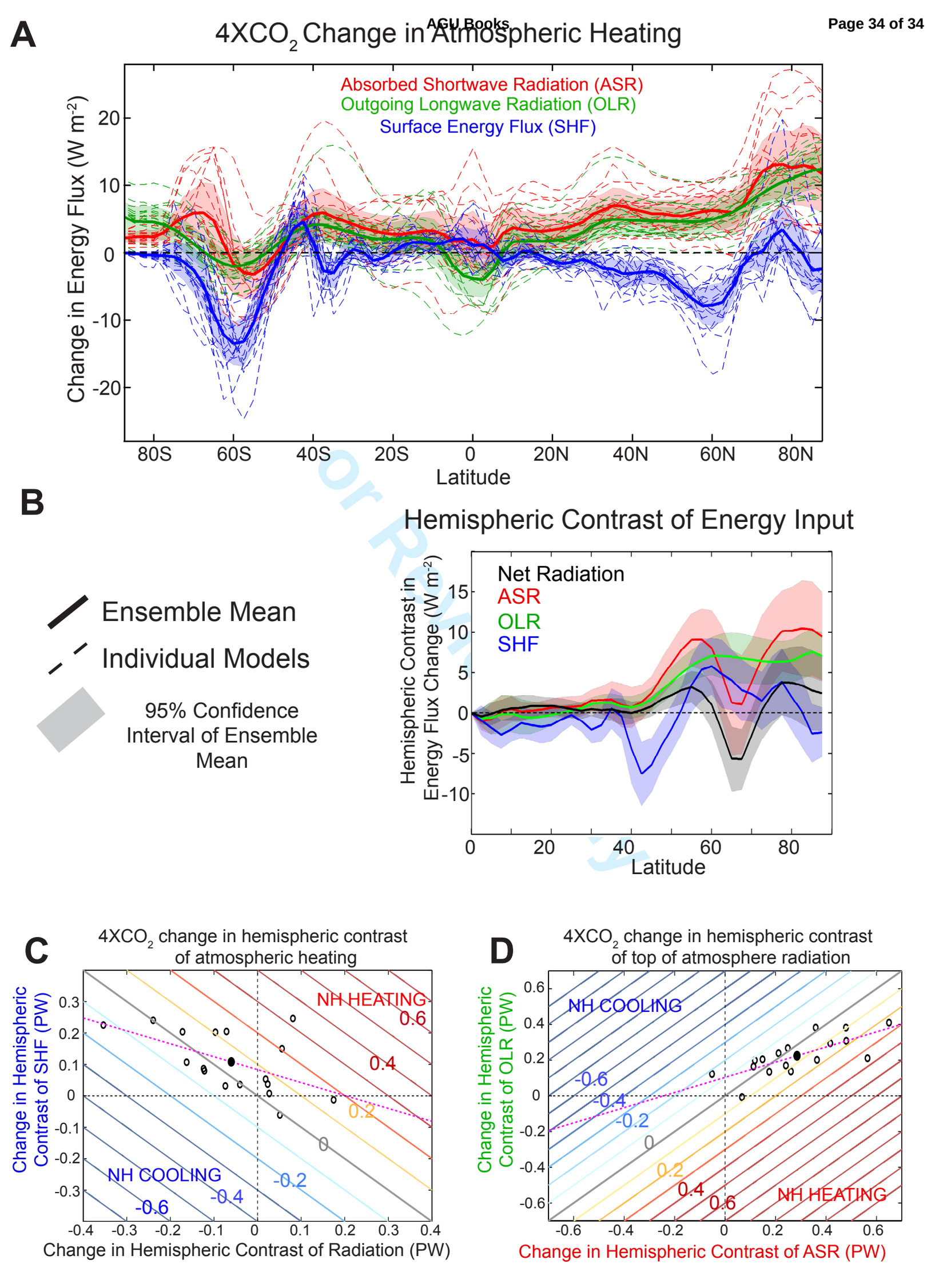
A
4XCO2 Change in Atmospheric Heating
Absorbed Shortwave Radiation (ASR)
Outgoing Longwave Radiation (OLR)
Surface Energy Flux (SHF)
Change in Energy Flux (W m-2)
20
10
0
-10
-20
80S
60S
40S
20S
0
20N
40N
60N
80N
Latitude
B
Hemispheric Contrast of Energy Input
Ensemble Mean
Individual Models
95% Confidence Interval of Ensemble Mean
Net Radiation
ASR
OLR
SHF
Hemispheric Contrast in Energy Flux Change (W m-2)
15
10
5
0
-5
-10
0
20
40
60
80
Latitude
C
4XCO2 change in hemispheric contrast of atmospheric heating
NH HEATING
0.6
0.4
0.2
0
NH COOLING
-0.2
-0.4
-0.6
Change in Hemispheric Contrast of SHF (PW)
0.3
0.2
0.1
0
-0.1
-0.2
-0.3
-0.4
-0.3
-0.2
-0.1
0
0.1
0.2
0.3
0.4
Change in Hemispheric Contrast of Radiation (PW)
D
4XCO2 change in hemispheric contrast of top of atmosphere radiation
NH COOLING
-0.6
-0.4
-0.2
0
0.2
0.4
0.6
NH HEATING
Change in Hemispheric Contrast of OLR (PW)
0.6
0.4
0.2
0
-0.2
-0.4
-0.6
-0.6
-0.4
-0.2
0
0.2
0.4
0.6
Change in Hemispheric Contrast of ASR (PW)

CMIP5 ITCZ location and AHT_{EQ} in pre-industrial simulations and under $4XCO_2$